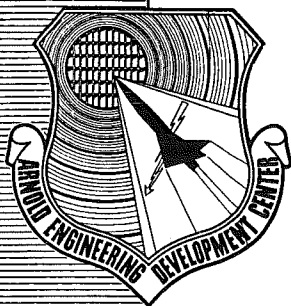


AEDC-TDR-62-7

*copy 1*

**ARCHIVE COPY  
DO NOT LOAN**



**METHODS OF APPROXIMATING INVISCID JET  
BOUNDARIES FOR HIGHLY UNDEREXPANDED  
SUPERSONIC NOZZLES**

By

J. R. Henson and J. E. Robertson  
Propulsion Wind Tunnel Facility  
ARO, Inc.

**TECHNICAL DOCUMENTARY REPORT NO. AEDC-TDR-62-7**

PROPERTY OF U.S. AIR FORCE  
AEDC TECHNICAL LIBRARY

**May 1962**

PROPERTY OF U.S. AIR FORCE  
AEDC LIBRARY  
AF 40(600) 800

(Prepared under Contract No. AF 40(600)-800 S/A 24(61-73) by ARO, Inc.,  
contract operator of AEDC, Arnold Air Force Station, Tennessee)

*Approved for public release; distribution unlimited.*

**ARNOLD ENGINEERING DEVELOPMENT CENTER  
AIR FORCE SYSTEMS COMMAND  
UNITED STATES AIR FORCE**

AEDC TECHNICAL LIBRARY



5 0720 00040 4113

# ***NOTICES***

Qualified requesters may obtain copies of this report from ASTIA. Orders will be expedited if placed through the librarian or other staff member designated to request and receive documents from ASTIA.

When Government drawings, specifications or other data are used for any purpose other than in connection with a definitely related Government procurement operation, the United States Government thereby incurs no responsibility nor any obligation whatsoever; and the fact that the Government may have formulated, furnished, or in any way supplied the said drawings, specifications, or other data, is not to be regarded by implication or otherwise as in any manner licensing the holder or any other person or corporation, or conveying any rights or permission to manufacture, use, or sell any patented invention that may in any way be related thereto.

METHODS OF APPROXIMATING INVISCID JET  
BOUNDARIES FOR HIGHLY UNDEREXPANDED  
SUPERSONIC NOZZLES

By

J. R. Henson and J. E. Robertson

Propulsion Wind Tunnel Facility

ARO, Inc.,

a subsidiary of Sverdrup and Parcel, Inc.

Approved for public release; distribution unlimited.

May 1962

**FOREWORD**

The authors would like to acknowledge the assistance of R. Pinkerton, North Carolina State College, Consultant, ARO, Inc., in developing the supersonic external flow method discussed in Section 2.4 of this report, and also the assistance of R. L. Hamner, PWT, for providing the experimental data discussed in Section 3.

**ABSTRACT**

Methods of approximating inviscid boundaries of jets exhausting from axisymmetric supersonic nozzles into a quiescent atmosphere and moving streams have been developed. Jet shapes from two typical afterbody configurations were calculated for various flight conditions. Good agreement with available theoretical and experimental data was obtained. A step-by-step calculational procedure is given in the Appendix.

## CONTENTS

	<u>Page</u>
ABSTRACT . . . . .	iii
NOMENCLATURE . . . . .	vii
1.0 INTRODUCTION . . . . .	1
2.0 ANALYSIS	
2.1 Quiescent Atmospheric Conditions. . . . .	3
2.2 Hypersonic External Flow - Configuration 1. . . . .	6
2.3 Hypersonic External Flow - Configuration 2. . . . .	8
2.4 Supersonic External Flow . . . . .	9
3.0 EXPERIMENTAL INVESTIGATION	
3.1 Tunnel Description . . . . .	11
3.2 Model Description. . . . .	11
3.3 Data Analysis . . . . .	11
4.0 DISCUSSION	
4.1 Comparison with Theory . . . . .	12
4.2 Comparison with Experimental Data. . . . .	12
4.3 Effects of Various Parameters . . . . .	14
4.4 Limitations. . . . .	14
5.0 CONCLUDING REMARKS. . . . .	15
REFERENCES . . . . .	16
APPENDIX . . . . .	17

## ILLUSTRATIONS

Figure

1. Schematic of Model Configurations	
a. Configuration 1 . . . . .	25
b. Configuration 2 . . . . .	25
2. Pressure Ratio and Mach Number versus Jet Radius between Two Points on a Boundary, (n) and (n + 1) . . . . .	26
3. Initial Angle Plot . . . . .	27
4. Schematic of Test Models	
a. $D/D_j = 1.0, M_j = 2.5$ . . . . .	28
b. $D/D_j = 2.0, M_j = 3.7$ . . . . .	28
5. Typical Schlieren Photograph of the Jet Structure, $M_\infty = 5.0$ . . . . .	29

<u>Figure</u>	<u>Page</u>
6. Jet Boundaries Calculated by the Present Quiescent Method Compared with the Method of Characteristics Solution and Latvala's Solution for a Quiescent Atmosphere . . . . .	30
7. Jet Boundaries Calculated by the Present Hypersonic Method Compared with the Method of Characteristics Solution	
a. Boundary Comparison, $M_\infty = 4.0$ . . . . .	31
b. Boundary Comparison, $M_\infty = 5.0$ . . . . .	32
c. Boundary Comparison, $M_\infty = 6.0$ . . . . .	33
8. Jet Boundaries Calculated by the Present Hypersonic Method Compared with Experimental Jet Shocks	
a. $M_\infty = 4.0$ . . . . .	34
b. $M_\infty = 5.0$ . . . . .	35
9. Jet Boundaries Calculated by the Present Methods Compared with Experimental Boundaries, $M_\infty = 3.5$	
a. $p_j/p_\infty = 10$ , $p_c/p_j = 101$ . . . . .	36
b. $p_j/p_\infty = 15$ , $p_c/p_j = 101$ . . . . .	37
10. Jet Boundaries Calculated by the Present Methods Compared with Experimental Boundaries, $M_\infty = 4.0$	
a. $p_j/p_\infty = 13.3$ , $p_c/p_j = 101$ . . . . .	38
b. $p_j/p_\infty = 20.0$ , $p_c/p_j = 101$ . . . . .	39
11. Jet Boundaries Calculated by the Present Methods Compared with Experimental Boundaries, $M_\infty = 5.0$	
a. $p_j/p_\infty = 35$ , $p_c/p_j = 101$ . . . . .	40
b. $p_j/p_\infty = 52$ , $p_c/p_j = 101$ . . . . .	41
12. Comparison of Jet Boundaries Calculated by the Present Hypersonic Method for Configurations 1 and 2 . . . . .	42
13. Jet Boundaries Calculated by the Present Methods for Various Free-Stream Mach Numbers	
a. Configuration 1 . . . . .	43
b. Configuration 2 . . . . .	44
14. Jet Boundaries Calculated by the Present Hypersonic Method for Various Nozzle Mach Numbers	
a. Configuration 1 . . . . .	45
b. Configuration 2 . . . . .	46
15. Jet Boundaries Calculated by the Present Hypersonic Method for Various Static Pressure Ratios, $p_j/p_\infty$	
a. Configuration 1 . . . . .	47
b. Configuration 2 . . . . .	48

<u>Figure</u>		<u>Page</u>
16.	Initial Angle Plot for Constant Nozzle Area Ratio, Chamber Pressure, and Free-Stream Altitude at Various Jet Specific Heat Ratios and Free-Stream Mach Numbers . . . . .	49
17.	Jet Boundaries Calculated by the Present Hypersonic Method for Various Jet Specific Heat Ratios	
	a. Configuration 1 . . . . .	50
	b. Configuration 2 . . . . .	51

## 1.0 INTRODUCTION

A jet exhausting from an underexpanded supersonic nozzle expands rapidly about the nozzle lip and forms a plume of complicated aerodynamic structure. The boundary of the plume is a mixing region resulting from the viscous interaction of the jet with the surrounding medium. In order to simplify the problem, the jet gas and the external gas in the mixing region may be assumed to lie in separate areas internally and externally, respectively, to a nonviscous streamline. Such an analogy is possible since the total mixing region acts as a nonviscous streamline of finite thickness - separating the jet and the surrounding medium.

A number of experimental and theoretical studies have been reported on the spreading of underexpanded jets exhausting into a quiescent atmosphere based on the above analysis of the jet boundary. However, only a few have considered the case of external flow. The method of characteristics is a technique available for the calculation of the jet structure. The characteristics solution reported by Wang and Peterson (Ref. 1) for jet spreading in a hypersonic stream utilizes Newton's impact equation to determine the pressure variation along the jet boundary caused by the interaction with the external stream. With the boundary conditions determined, the method of characteristics can be readily applied to calculate the jet flow field. However, the computations are lengthy and require electronic computing equipment. To avoid the complications of the characteristics solution, Latvala (Ref. 2) and Adamson and Nicholls (Ref. 3) replaced the effects of expansion waves impinging on the jet boundary by a quasi one-dimensional area increase, and developed a simplified method of estimating jet spreading into a quiescent atmosphere.

The present study adapts Newton's impact theory as in Wang and Peterson's solution and the conical flow theory as applied to the flow about bodies of revolution to a one-dimensional flow solution. The results are simple approximate solutions for estimating the boundaries of jets expanding into either a quiescent atmosphere or an external flow.

Satisfactory comparison with theoretical results obtained by the characteristics solution and Latvala's solution are shown for the quiescent atmosphere condition. Only a limited amount of jet spreading data with external flow was available for comparison with the methods suggested here; however, satisfactory comparisons were made which should justify the use of the methods for further studies.

## 2.0 ANALYSIS

The present analysis of a supersonic jet expanding into a quiescent atmosphere or a high velocity stream employs some of the principal assumptions and equations used by Wang and Peterson (Ref. 1) and Latvala (Ref. 2)

In the case of an underexpanded nozzle, there are expansion waves originating at the nozzle lip and propagating downstream toward the jet boundary. These waves impinge on the boundary, turn the flow, and are reflected as compression waves. The compression waves then converge to form a finite shock wave. The method of characteristics reported by Wang and Peterson is based on this analysis of the jet structure.

The present methods and the method developed by Latvala depend on replacing the effects of expansion waves impinging on the jet boundary flow by one-dimensional flow relations. However, the present method is different from Latvala's method in that Newtonian theory is used in conjunction with one-dimensional flow theory to define the jet structure. By one-dimensional theory, as the area of the expanding jet increases downstream of the nozzle exit, the internal boundary pressure decreases. To maintain boundary equilibrium, the boundary flow direction changes, retarding the expansion of the jet. Compression waves generated from the boundary converge to form a shock originating immediately downstream of the nozzle lip. The shock structure is analogous to the structure described above for the method of characteristics. For jet boundary Mach numbers in the hypersonic range, the boundary shock is close to the boundary streamline (see photographs in Ref. 2). Therefore, there will be very little flow across the shock, and the Newtonian impact theory is justified for the internal jet flow as is the assumption of an isentropic flow field. In the present analysis, only the case where the internal flow near the boundary was in or near the hypersonic range ( $M_b \geq 4.0$ ) was considered. However, for the case where the flow near the boundary is in the supersonic range, it may be possible to incorporate oblique shock relations.

Two typical afterbody configurations are considered. For Configuration 1 the nozzle exit diameter is equal to the model base diameter (Fig. 1a), whereas for Configuration 2 the nozzle exit diameter is smaller than the model base diameter (Fig. 1b). Although there are many different base configurations, the most typical may be grouped into these two basic categories. The afterbody configuration does not influence the boundary of a jet expanding into a quiescent atmosphere; however, its influence is appreciable for external flow.

## 2.1 QUIESCENT ATMOSPHERIC CONDITIONS

When a jet is exhausting into a quiescent atmosphere, it may be assumed that the pressure along the external boundary remains constant and is equal to that of the ambient conditions. By one-dimensional flow relations, the internal flow will vary between points on the boundary. Consequently, only one set of flow equations representing the internal jet conditions is necessary to describe the jet boundary.

The initial expansion of the jet will follow Prandtl-Meyer flow as outlined in Refs. 2 and 3. The expansion is complete when the pressure on the jet boundary has reached the ambient conditions. Prandtl-Meyer equations may be used to represent the initial expansion of the internal flow

$$\alpha_1 = \nu_1 - \nu_j + \theta_N \quad (1)$$

where

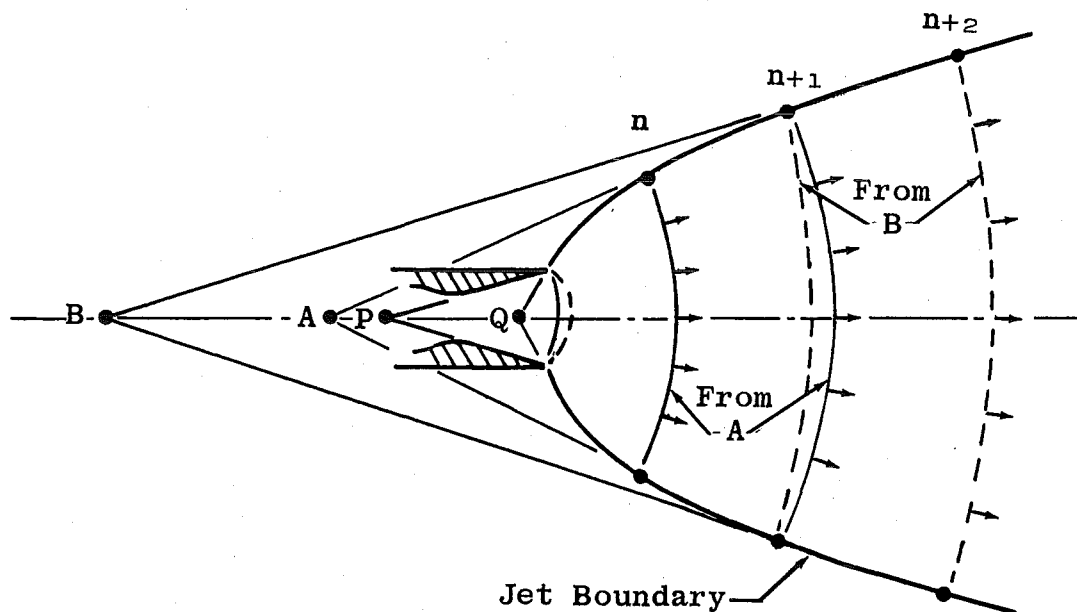
$$\nu_1 = f \left( \frac{P_{b_1}}{P_c} \right), \quad P_{b_1} = P_\infty$$

$$\nu_j = f \left( \frac{P_j}{P_c} \right)$$

The notation employed in Eq. (1) is indicated in Fig. 1a.

The shape of the jet boundary downstream of the nozzle exit may be approximated by considering quasi one-dimensional area increases of the jet. That is, it may be assumed that one can find the Mach number and pressure at any axial position in an expanding flow from the area ratio at a given point. Therefore,  $(A/A^*)_1$  corresponding to  $(p_\infty/p_c)$  can be obtained from compressible flow tables based on the specific heat ratio of the exhausting jet. By beginning with  $\alpha_1$  and  $(A/A^*)_1$  at the nozzle lip, a point-by-point calculation along the jet boundary can be made.

To determine the jet boundary shape it is necessary to assume a one-dimensional area increase of the jet over a finite distance between a point on the boundary denoted by (n) at a radius  $(r_n)$  and a nearby point (n + 1) at a radius  $r_n + \Delta r$ . Flow conditions within the jet are assumed to be constant over a spherical surface, illustrated on the following page as a circular arc, centered at the hypothetical source A.



The smaller the value used for  $\Delta r$  the better will be the approximation. With  $\alpha_n$  calculated and  $\Delta r$  assumed between (n) and (n + 1) the boundary point (n + 1) may be located by

$$\frac{r_{n+1}}{r_j} = \frac{r_n}{r_j} + \frac{\Delta r}{r_j} \quad (2)$$

$$\frac{x_{n+1}}{r_j} = \frac{x_n}{r_j} + \frac{\Delta x}{r_j} = \frac{x_n}{r_j} + \frac{\Delta r \cot \alpha_n}{r_j} \quad (3)$$

The external ambient pressure is constant between (n) and (n + 1), whereas the internal pressure has decreased corresponding to one-dimensional flow relations. At (n + 1) the boundary is no longer in equilibrium. To balance the pressure internally and externally, it is necessary to decrease the angle of the boundary at (n + 1), compressing the flow near the boundary to the ambient pressure. With the resulting angle  $\alpha_{n+1}$  one may define a new hypothetical source B as shown in the sketch. The jet flow field is then assumed to be related to the ambient pressure which exists both internally and externally to the jet boundary immediately aft of the point (n + 1). Beginning with the new flow conditions  $\alpha_{n+1}$  and  $(A/A^*)$  (corresponding to  $p_\infty/p_c$ ) one may now assume a one-dimensional area increase from (n + 1) to (n + 2) with B as the hypothetical source. This analysis is similar to that used at the nozzle exit. As the jet expands about the nozzle lip to the ambient pressure, the value of  $(A/A^*)$  increases correspondingly. During the expansion the hypothetical source moves from P to Q.

To determine the resulting angle  $\alpha_{n+1}$  the assumption is made that the varying internal flow between (n) and (n + 1) may be represented by

average flow conditions between these two points if the corresponding radius change is small. This approximation is analogous to that employed in the generalized shock expansion method, Ref. 4, where curved body shapes are approximated by a series of conical frustums. In this analysis it allows the flow at the point (n) to be simply related to the flow at point (n + 1). Since the jet flow of a highly underexpanded nozzle is in or near the hypersonic range ( $M_b \geq 4.0$ ), the Newtonian impact equation may be applied to the internal flow. Employing Newtonian theory and representing the flow near the boundary over a small interval by the average conditions in the interval results in the following equation.

For the internal flow the dimensionless Newtonian impact equation is

$$\frac{p_{b_{n+1}}}{p_c} = \frac{(p_b)_{avg}}{p_c} \left[ \gamma_j (M_b)_{avg}^2 \sin^2 (\alpha_n - \alpha_{n+1}) + 1 \right] \quad (4)$$

where  $p_{b_{n+1}} = p_\infty$  for the quiescent atmosphere case.

From Eq. (4) the new angle is

$$\alpha_{n+1} = \alpha_n - \sin^{-1} \sqrt{\frac{\frac{p_\infty}{p_c} - \frac{(p_b)_{avg}}{p_c}}{\frac{(p_b)_{avg}}{p_c} \gamma_j (M_b)_{avg}^2}} \quad (4a)$$

The average internal flow conditions between (n) and (n + 1) correspond to the average Mach number between (n) and (n + 1), assuming the Mach number varies linearly with jet radius. Mach number was used as a basis for the average flow conditions rather than pressure since the change in Mach number for change in jet radius is more nearly linear (see Fig. 2). This assumption is reasonable for small  $\Delta r$ . The average Mach number may be calculated from

$$(M_b)_{avg} = \frac{M_{b_n} + M_{b_{n+1}}}{2} \quad (5)$$

$M_{b_n}$  and  $M_{b_{n+1}}$  correspond to  $(A/A^*)_n$  and  $(A/A^*)_{n+1}$ .  $(A/A^*)_n$  is known and  $(A/A^*)_{n+1}$  may be calculated as follows:

$$\left(\frac{A}{A^*}\right)_{n+1} = \frac{(r_{n+1})^2}{(r_n)^2} \left(\frac{A}{A^*}\right)_n \quad (6)$$

From compressible flow tables based on  $\gamma_j$ ,  $(p_b)_{avg}/p_c$  corresponding to  $(M_b)_{avg}$  may be obtained.

An approximate nearby boundary point ( $n + 2$ ) may now be located by assuming the boundary flow angle,  $\alpha_{n+1}$ , to be constant from ( $n + 1$ ) to ( $n + 2$ ). The location is given by Eqs. (2) and (3). This procedure is begun at the nozzle lip ( $n = 1$ ) and repeated application will provide a step-by-step estimation of the jet boundary.

To facilitate the use of this method, a step-by-step procedure is given in the Appendix.

A mathematically correct solution for calculating the jet boundary would be to apply the correction angle required to place the inviscid streamline in pressure equilibrium at ( $n + 1$ ) to the previous point ( $n$ ). However, it was found that this solution produced a more compressed jet boundary than actually exists. It is shown later, in comparisons with experimental boundaries, that the presented methods result in very good agreement. An explanation for the greater expansion of the experimental jet may be credited to the initial overexpansion of the jet about the nozzle lip. Also, for the case of external flow, the compression caused by the free stream impinging on the jet was assumed to be instantaneous at a point; whereas, the compression actually takes place over a small interval.

It is interesting to note that the final results of applying the corrected streamline angle at ( $n + 1$ ) instead of ( $n$ ) will differ from zero at the nozzle lip to the  $\Delta r$  value at the maximum jet diameter ( $\alpha = 0$ ). This indicates that the two methods are essentially equivalent for sufficiently small values of  $\Delta r$ .

## 2.2 HYPERSONIC EXTERNAL FLOW - CONFIGURATION I

The shape of a jet boundary which is exposed to an external stream is influenced by the flow conditions both internal and external to the jet. Consequently, two sets of flow equations, one representing the internal jet conditions and the other representing the external flow, are necessary to describe the jet boundary. Variables satisfying both the internal and external flow equations simultaneously specify the boundary.

Similar to the expansion of a jet into a quiescent atmosphere, the initial expansion of the jet into an external stream will follow Prandtl-Meyer flow. The expansion is complete when the pressure on the jet boundary is in equilibrium with the surrounding medium. As before, Eq. (1) may be used to represent the initial expansion of the internal flow:

$$\alpha_i = \nu_i - \nu_j + \theta_N$$

where

$$\nu_1 = f \left( \frac{P_{b1}}{P_c} \right)$$

$$\nu_j = f \left( \frac{P_j}{P_c} \right)$$

When a jet is issuing into a moving stream, the boundary pressure is no longer constant and the interaction between the jet and the external stream must be taken into account. As far as the external flow is concerned, the jet may be treated as a solid body, and with a hypersonic external flow, Newtonian theory can be used. The dimensionless Newtonian impact equation representing the external boundary conditions at the nozzle lip ( $n = 1$ ) is defined by

$$\frac{P_{b_n}}{P_c} = \frac{P_\infty}{P_c} \left[ \gamma_\infty M_\infty^2 \sin^2 \alpha_n + 1 \right] \quad (7)$$

The initial expansion equation and Eq. (7) are both functions of  $\alpha_1$  and  $p_{b1}/p_c$ . Upon leaving the nozzle exit, the flow about the lip will expand to the angle  $\alpha_1$  and to the boundary pressure,  $p_{b1}$ . It is evident that only one pair of values of  $\alpha_1$  and  $p_{b1}/p_c$  will define the initial portion of the boundary. These values may be determined by simultaneously solving Eqs. (1) and (7), either analytically or graphically, as shown in Fig. 3 for the flow conditions used by Wang and Peterson (Ref. 1).

The boundary shape is determined by an analysis similar to that used for the quiescent atmospheric condition. The boundary flow direction is assumed to remain constant from ( $n$ ) to ( $n + 1$ ) and, knowing  $\alpha_n$  and assuming some  $\Delta r$ , the nearby boundary point ( $n + 1$ ) is defined by Eqs. (2) and (3). To locate the boundary point ( $n + 2$ ), the boundary angle at ( $n + 1$ ) must be calculated. This is done by again assuming that the varying internal flow between ( $n$ ) and ( $n + 1$ ) may be represented by the average flow conditions between these two points. The average conditions corresponding to the average Mach number between ( $n$ ) and ( $n + 1$ ) are calculated as described for the quiescent external conditions. Since the external Mach number,  $M_\infty$ , and the jet boundary Mach number,  $(M_b)_{avg}$ , are both assumed in the hypersonic range, the dimensionless Newtonian impact equation (Eq. (7)) may be used to determine the flow conditions necessary to restore the external and internal flow to equilibrium at ( $n + 1$ ).

For the internal flow, Eq. (4) is used:

$$\frac{P_{b_{n+1}}}{P_c} = \frac{(P_b)_{avg}}{P_c} \left[ \gamma_j (M_b)_{avg}^2 \sin^2(\alpha_n - \alpha_{n+1}) + 1 \right]$$

whereas for the external flow, Eq. (7) is used:

$$\frac{P_{b_{n+1}}}{P_c} = \frac{P_\infty}{P_c} \left[ \gamma_\infty M_\infty^2 \sin^2 \alpha_{n+1} + 1 \right]$$

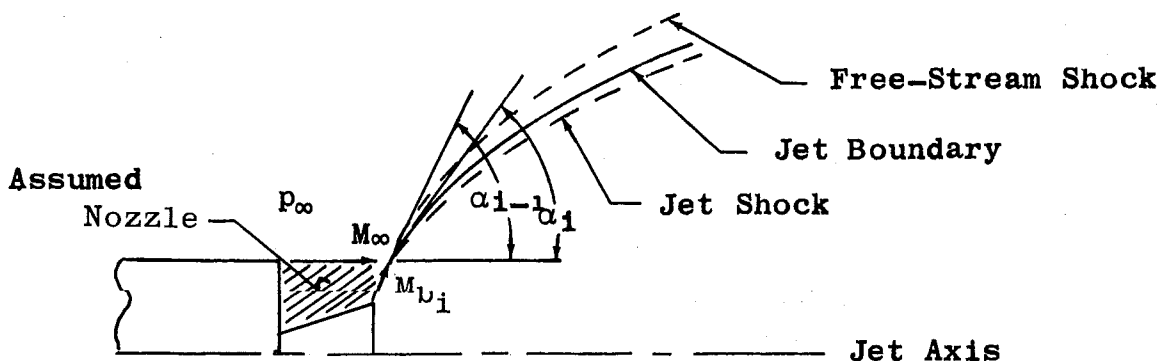
Free-stream pressure is determined from external flow conditions.

From the two equations the angle of flow,  $\alpha_{n+1}$ , can be obtained by graphical methods. By again assuming one-dimensional flow between  $(n+1)$  and  $(n+2)$  for some  $\Delta r$ , the boundary point  $(n+2)$  may be located by Eqs. (2) and (3). This procedure is begun at the nozzle lip and is repeated at each boundary point.

### 2.3 HYPERSONIC EXTERNAL FLOW - CONFIGURATION 2

In analyzing the jet spreading for Configuration 2 (see Fig. 1b), the free stream was assumed to remain parallel to the jet axis from the missile base to the point of intersection with the jet boundary. With this assumption, the base pressure would be equal to the free-stream pressure and remain constant along the boundary from the nozzle lip to the point of intersection. If, however, the missile base pressure is known or can be determined, the turning of the free stream at the base may be calculated and the point of intersection accurately located. At hypersonic velocities the base pressure approaches the free-stream pressure, and subsequent turning of the free stream would be small.

The initial portion of the boundary from the nozzle lip to the point of intersection with the external stream is assumed to be a boundary with constant external pressure and may be determined as described for the quiescent condition. At the point of impact the external stream begins to retard the jet expansion and the boundary pressure is no longer constant. It may then be assumed that the flow conditions at the point of intersection are similar to the flow conditions about the lip of an over-expanded hypersonic nozzle, as illustrated below.



If the external Mach number,  $M_\infty$ , and the jet Mach number,  $(M_b)_{avg}$ , at the point of intersection are both in the hypersonic range, the impact equation may be used to determine the boundary pressure caused by internal and external flow at the intersection of both streams.

For the internal flow, Eq. (4) is applicable ( $n = i-1$ )

$$\frac{p_{bi}}{p_c} = \frac{(p_b)_{avg}}{p_c} \left[ \gamma_j (M_b)_{avg}^2 \sin^2 (\alpha_{i-1} - \alpha_i) + 1 \right]$$

where  $(M_b)_{avg} = \frac{M_{bi-1} + M_{bi}}{2}$  and  $\frac{(p_b)_{avg}}{p_c}$  corresponds to  $(M_b)_{avg}$ . (See the analysis on average internal flow conditions as described in section 2.1.)

For the external flow, Eq. (7) is used:

$$\frac{p_{bi}}{p_c} = \frac{p_\infty}{p_c} \left[ \gamma_\infty M_\infty^2 \sin^2 \alpha_i + 1 \right]$$

These two equations specify the angle of the flow,  $\alpha_i$ , and the pressure,  $p_{bi}$ , at the intersection point of the jet and the free stream. The new value of  $M_{bi}$  can then be obtained as a function of  $p_{bi}/p_c$ . Calculations of subsequent points are the same as for Configuration 1 using the conditions calculated after intersection has occurred.

To facilitate the use of this method for both configurations, a step-by-step procedure is given in the Appendix.

## 2.4 SUPERSONIC EXTERNAL FLOW

When a jet is issuing into a supersonic stream, the external boundary pressure may no longer be defined by Newtonian theory. The present approximation involves compressing the free stream through a conical shock created by the interaction of the free stream with the jet at the nozzle lip. Aft of the shock, the external flow is defined by a series of small angle Prandtl-Meyer expansions about the jet boundary.

The pressure coefficient equation is

$$C_p = \frac{p_{b1} - p_\infty}{q_\infty} = \frac{2}{\gamma_\infty M_\infty^2} \left[ \frac{p_{b1}}{p_\infty} - 1 \right] \quad (8)$$

where  $C_p = f(\alpha_1, M_\infty)$  (defined from conical flow charts).

Rearranging Eq. (8) the initial boundary pressure ratio may be expressed as a function of the free-stream conditions:

$$\frac{P_{b1}}{P_c} = \frac{P_\infty}{P_c} \left[ \frac{\gamma_\infty M_\infty^2}{2} C_p + 1 \right] \quad (8a)$$

The initial expansion of the jet follows Prandtl-Meyer flow, as previously discussed. Unique values of the initial flow conditions ( $\alpha_1$  and  $P_{b1}/P_c$ ) may be determined by simultaneously solving Eqs. (1) and (8a) either analytically or graphically.

The boundary shape is determined by an analysis similar to that used for the hypersonic external flow case. The difference is in the definition of the external boundary pressure.

For the external flow,

$$\nu_{\infty_{n+1}} = \nu_{\infty_n} + (\alpha_n - \alpha_{n+1}) \quad (9)$$

where

$$\frac{P_{b_{n+1}}}{P_t} = f(\nu_{\infty_{n+1}}) \quad \text{and} \quad \frac{P_{b_{n+1}}}{P_c} = \frac{P_{b_{n+1}}}{P_t} \left( \frac{P_{b_n}}{P_c} \right) \left( \frac{P_t}{P_{b_n}} \right)$$

For the internal flow, Eq. (4) is used:

$$\frac{P_{b_{n+1}}}{P_c} = \frac{(P_b)_{avg}}{P_c} \left[ \gamma_j (M_b)_{avg}^2 \sin^2 (\alpha_n - \alpha_{n+1}) + 1 \right]$$

From the above equations, an incremental analysis of the boundary is made, beginning with the initial conditions at the nozzle lip.

The analysis of the jet boundary for Configuration 2 is also similar to the corresponding analysis for hypersonic external flow. The quietest calculations are used to determine the initial portion of the boundary to the point of intersection with the external stream. At the intersection, assuming an overexpanded nozzle to exist, the supersonic flow method as described in this section is incorporated to continue along the boundary.

To facilitate the use of this method for both configurations, a step-by-step procedure is given in the Appendix.

### 3.0 EXPERIMENTAL INVESTIGATION

Experimental data used in the present study were obtained from wind tunnel tests conducted by the Research and Performance Branch,

Propulsion Wind Tunnel Facility (PWT), in the 12-in. Supersonic Tunnel of the von Kármán Gas Dynamics Facility (VKF) at the Arnold Engineering Development Center (AEDC).

### 3.1 TUNNEL DESCRIPTION

The 12-in. Supersonic Tunnel is an intermittent wind tunnel with a Mach number range from 1.5 to 5. Stagnation pressures are regulated with automatic control valves which throttle the flow from the air-storage system. Low discharge pressures are maintained by means of a vacuum sphere. For a more detailed description of the 12-in. Supersonic Tunnel and its operating parameters see Ref. 5.

### 3.2 MODEL DESCRIPTION

Two high pressure, cold-flow model configurations were investigated (see Fig. 4). A model of boattail design representing a typical no-base afterbody is shown in Fig. 4a. The model consisted of a 2.0-in. -diam stainless-steel cylinder to which an ogive nose and interchangeable exit nozzles could be attached. In the present program only the complete, boattailed, 2.5 exit Mach number nozzle was investigated.

The model simulating an afterbody configuration with a model base diameter larger than the nozzle exit diameter (see Fig. 4b) consisted of a 2.0-in. stainless-steel cone-cylinder to which interchangeable nozzles could be attached. In the present study only the 3.7 exit Mach number nozzle was investigated.

### 3.3 DATA ANALYSIS

Experimental data used in comparison with the present method were obtained by the schlieren photographic and shadowgraph processes. The knife edge for schlieren photographs in this report was oriented such that positive density gradients in a vertical downward direction appear as dark regions on the photograph.

A typical schlieren photograph of a jet issuing from a supersonic nozzle into a hypersonic free stream is given in Fig. 5. The boundary of the jet is defined by a mixing region, as noted on the photograph. The density gradient of the mixing boundary normal to the knife edge is positive, as indicated by the darkness of the photograph.

The free stream impinging on the mixing boundary is initially compressed through a conical shock and then expands about the boundary similar to flow about a body of revolution. The density gradient across the shock normal to the knife edge is positive and appears as a dark region on the schlieren photograph. The expansion of the free stream aft of the shock creates a negative density gradient normal to the knife edge and appears as a light region on the schlieren photograph.

Internal to the mixing boundary is a shock formed by expansion waves from the nozzle reflecting from the boundary as compression waves. Jet flow passing through the shock is compressed, creating a negative density gradient normal to the knife edge. The corresponding area in Fig. 5 is light, as noted.

A shadowgraph of the jet structure may be analyzed similar to that above, noting that a shadowgraph measures rate of change of density gradient.

#### 4.0 DISCUSSION

##### 4.1 COMPARISON WITH THEORY

Boundaries calculated by the present method for quiescent atmospheric conditions are compared with theoretical boundaries obtained by the method of characteristics and Latvala's solution (results taken from Ref. 2) in Fig. 6. Close agreement was obtained at pressure ratios ( $p_j/p_\infty$ ) of 81 and above. A deviation of boundaries was obtained at a pressure ratio ( $p_j/p_\infty$ ) of 10, with the present solution giving the smaller boundary.

Figure 7 presents a comparison of the present hypersonic method with the characteristics solution by Wang and Peterson at free-stream Mach numbers of 4, 5, and 6. Boundaries calculated by the hypersonic method give about 15 percent less expansion in radius than the characteristics solution. The pressure at points on the boundary caused by external flow is calculated using Newton's impact equation in both methods; however, computations to correct the internal conditions for the change in external pressure are considerably different, as described in the analysis.

##### 4.2 COMPARISON WITH EXPERIMENTAL DATA

Jet boundaries calculated by the present method and in Refs. 1 through 3 are for inviscid flow and essentially represent dividing streamlines between the jet and external stream. When these inviscid boundaries

are compared with experimental boundaries, they should obviously lie within the viscous mixing region (see Fig. 5); however, their exact relation to the mixing region is not known unless some characteristic mixing profile is measured. In order to relate computed boundaries to physical viscous flows, the nonviscous streamlines have been used to compute theoretical jet shocks which then can be directly compared with experimental jet shocks. The method of estimating the shock location is contained in Ref. 6. It consists of determining the local Mach line at each calculated boundary point for the jet flow. When these Mach lines are graphically located, they coalesce into the theoretical jet shock.

Boundaries with which to compare the present hypersonic method for Configuration 1 were obtained with a model of boattail design (see Fig. 4a). The external flow was assumed to be equal to free-stream tunnel conditions on the cylindrical portion of the model, and then expanded (by Prandtl-Meyer theory) through the angle of the boattail prior to impinging on the jet. Calculations were then made as described for Configuration 1. Experimental data for external Mach numbers of 4 and 5 were taken from shadowgraphs. Because of the poor quality of the shadowgraphs, only the jet shocks could be identified. Boundaries were calculated by the hypersonic method, and from the boundaries theoretical jet shocks were constructed. The present solutions are compared with the experimental jet shocks in Fig. 8. Excellent agreement with the jet shocks in Fig. 8 seem to indicate that the calculated nonviscous streamlines are correctly located in the boundary mixing region. The initial portion of the jet shocks in Fig. 8a could not be clearly identified for an axial distance of approximately two nozzle diameters aft of the nozzle exit. However, good agreement over the identifiable portion was obtained.

Experimental data to compare both the hypersonic and supersonic methods for Configuration 2 were obtained from schlieren photographs. Base pressures from four orifices located in the model base region were used to correctly locate the interaction of the jet boundary and the free stream. The pressure readings were averaged and the external flow - assumed to be equal to free-stream tunnel conditions on the model afterbody - was expanded or compressed to satisfy base conditions. Calculations to determine the boundary streamline were then made as described in the analysis. Boundaries calculated by the present methods and the corresponding jet shocks are compared with experimental jet structures in Figs. 9, 10, and 11 for various flight conditions. Good agreement with the shock was obtained over the initial portion of the jet. It should be noted that aft of the maximum diameter of the experimental jet shock, the calculated shock does not agree as well with experiment

(see Figs. 9 and 10). This indicates that the assumption of one-dimensional flow field becomes less valid with increasing divergence of the jet shock and the jet boundary.

Comparisons of both the hypersonic and supersonic methods with experimental boundaries were made at free-stream Mach numbers of 3.5, 4.0, and 5.0 (see Figs. 9b, 10b, and 11b). Very close agreement of the two methods was obtained for this Mach number range. Additional comparisons of boundaries for free-stream Mach numbers of 2.5 and 8.0 were made (comparisons not shown in report). The result was a deviation of 7.4 percent and 6.7 percent of the calculated boundary radii at 4 jet exit radii downstream of the jet exit for the two Mach numbers, 2.5 and 8.0, respectively. For both cases the hypersonic method predicted the larger boundary.

#### 4.3 EFFECTS OF VARIOUS PARAMETERS

The present methods were also used to study the effects of various parameters on jet spreading. Comparisons of calculated boundaries for the two typical afterbody configurations are presented in Fig. 12. As the base-to-nozzle exit diameter ratio increases, the jet spreading also increases. The effects of external Mach number, nozzle Mach number, and static pressure ratio,  $p_j/p_\infty$ , can be seen in Figs. 13, 14, and 15. It is apparent that jet spreading increases with either an increase in  $p_j/p_\infty$  or a decrease in nozzle Mach number, and decreases with an increase in external Mach number.

At constant values of nozzle area ratio, chamber total pressure, and altitude, as nozzle Mach number varies with specific heat ratio, the jet boundary will follow a definite pattern of change (see Figs. 16 and 17). The relative change in spreading is indicated by examination of the plot of the Prandtl-Meyer and Newtonian equations in Fig. 16. As the specific heat ratio decreases, the initial angle increases for a constant free-stream Mach number. The jet spreading also increases, as shown for an external Mach number of 5.0 in Fig. 17.

#### 4.4 LIMITATIONS

It should be pointed out that the present methods have certain inherent limitations because of the assumption of a one-dimensional jet flow field. In addition to this initial assumption, the following limitations exist: First, the present solutions do not give a means of calculating the mixing region of the jet boundary. Second, the supersonic

external flow method cannot be used when the external flow separates from the model afterbody prior to impinging on the jet boundary, unless the point and angle of separation are known or may be determined. Third, the boundary Mach number must be hypersonic in order to use Newtonian theory for the internal flow of the jet. Fourth, the solutions are based on a continuum theory; and lastly, the methods are only valid when the undisturbed free-stream flow is axisymmetric to the jet axis (model angle of attack of zero). It should be noted that with the exception of the first and fourth limitations, all concern special cases. Under practical operating conditions, the methods presented will produce a good approximation of the jet spreading.

Although the present method deals with equilibrium flow within the jet, it may be noted that a modification of the present method may possibly be used when the jet flow is not in equilibrium. If the  $\gamma_j$  distribution along the axis of the jet is known, or may be determined, the calculation over each increment on the boundary may be based on the corresponding  $\gamma_j$ . This technique would be based on equilibrium flow only over small increments of the jet.

## 5.0 CONCLUDING REMARKS

The present method, as used for quiescent external conditions, shows good agreement with the method of characteristics and the method introduced by Latvala (Ref. 2). A comparison of the present method with experimental data for a quiescent atmosphere was not deemed necessary since both the method by Latvala and the characteristics solution have previously shown good agreement with experimental data for the quiescent external condition.

A comparison of the supersonic and hypersonic methods with the characteristics solution for external Mach numbers of 4, 5, and 6 shows slightly lower boundaries, the difference in boundary diameter being less significant at the larger free-stream Mach numbers. However, the present method results for the case of supersonic and hypersonic external flow show close agreement with experimental data for both base configurations. Because of the lack of clarity of the experimental exhaust boundaries, taken from photographs, a comparison could only be made to 6 or 7 nozzle exit diameters downstream of the nozzle exit.

Comparisons of the supersonic and hypersonic methods with experimental boundaries for undisturbed free-stream Mach numbers of 3.5, 4.0, and 5.0 are in good agreement. For cases with low supersonic and high

hypersonic external conditions a slight deviation of the two methods resulted. Since no experimental boundaries in the low supersonic or high hypersonic free-stream range were available for comparisons, no definite conclusions could be made as to an upper or lower free-stream Mach number limit for either method. However, based on the results presented, either method should give a good approximation of jet boundaries from highly underexpanded supersonic nozzles.

It is interesting to note the effects of varying jet and free-stream conditions for boundaries calculated by the present methods. For constant nozzle geometry, chamber total pressure, and altitude, the jet spreading increases with decreasing specific heat ratio. Whereas, for constant specific heat ratio, the spreading increases with increasing altitude (increasing  $p_j/p_\infty$ ) and decreases with increasing nozzle exit Mach number (increasing  $p_c/p_j$ ).

#### REFERENCES

1. Wang, C. T. and Peterson, J. G. "Spreading of Supersonic Jets from Axially Symmetric Nozzles." American Rocket Society Preprint No. 462-57, 1957.
2. Latvala, E. K. "Spreading of Rocket Exhaust Jets at High Altitudes." AEDC-TR-59-11, June 1959.
3. Adamson, T. C., Jr. and Nicholls, J. A. "On the Structure of Jets from Highly Underexpanded Nozzles into Still Air." Journal of the Aeronautical Sciences, January 1959, pp. 16-24.
4. Eggers, A. J., Jr., Savin, Raymond, C., and Syvertson, Clarence A. "The Generalized Shock-Expansion Method and Its Application to Bodies Traveling at High Supersonic Airspeeds." Journal of the Aeronautical Sciences, Vol. 22, No. 4, April 1955, pp. 231-238.
5. Test Facilities Handbook, (3rd Edition). "Von Kármán Gas Dynamics Facility, Vol. 4." Arnold Engineering Development Center, January 1961.
6. Adamson, T. C., Jr. "Approximate Methods for Calculating the Structure of Jets from Highly Underexpanded Nozzles." The University of Michigan, Report No. 3768-26-T, June 1961.

## APPENDIX

## COMPUTATIONAL PROCEDURE - QUIESCENT ATMOSPHERE

Step 1

- a. Calculate the initial angle of jet boundary at the nozzle lip for a base pressure,  $p_{b1} = p_{\infty}$

$$\alpha_1 = \nu_1 - \nu_j + \theta_N$$

$\nu_1$  and  $\nu_j$  correspond to  $p_{b1}/p_c$  and  $M_j$ , respectively, and are obtained from compressible flow tables based on  $\gamma_j$ .  $\theta_N$  is known from the nozzle geometry.

- b. Locate Point 2 by assuming one-dimensional flow from the nozzle lip, Point 1, to some arbitrary Point 2 where from Eq. (2)

$$\frac{r_2}{r_j} = 1 + \frac{\Delta r}{r_j}$$

and from Eq. (3)

$$\frac{x_2}{r_j} = \frac{\Delta x}{r_j} = \frac{\Delta r \cot \alpha_1}{r_j}$$

Step 2

- a. To locate Point 3, find the average internal flow conditions between Points 1 and 2 and compress this flow to the free-stream static pressure at Point 2. The average internal flow conditions are calculated as follows:

1. Find  $(A/A^*)_1$  corresponding to  $p_{\infty}/p_c$  from the compressible flow tables representing the exhaust gas.
2. Calculate  $(A/A^*)_2$  from Eq. (6) as

$$\left(\frac{A}{A^*}\right)_2 = \left(\frac{r_2}{r_1}\right)^2 \left(\frac{A}{A^*}\right)_1 \quad r_1 = r_j$$

3. Find  $M_{b1}$  and  $M_{b2}$  corresponding to  $(A/A^*)_1$  and  $(A/A^*)_2$ , respectively, from the compressible flow tables for the  $\gamma$  of the exhaust gas.
4. Calculate  $(M_b)_{avg}$  between Points 1 and 2 by assuming a linear Mach number distribution over the finite distance between 1 and 2. From Eq. (5).

$$(M_b)_{avg} = \frac{M_{b1} + M_{b2}}{2}$$

5. Find  $(p_b/p_c)_{avg}$  corresponding to  $(M_b)_{avg}$  from the compressible flow tables representing  $\gamma_j$ .
- b. From Eq. (4a),  $\alpha_2$  is obtained as

$$\alpha_2 = \alpha_1 - \sin^{-1} \sqrt{\frac{\frac{p_\infty}{p_c} - \left(\frac{p_b}{p_c}\right)_{avg}}{\left(\frac{p_b}{p_c}\right)_{avg} \gamma_j (M_b)_{avg}^2}}$$

$\alpha_1$  is known from Step 1.

- c. With  $\alpha_2$  determined, Point 3 may be located by assuming one-dimensional flow from Points 2 to 3 (same operation as in Step 1b using Eqs. (2) and (3)).

Subsequent points along the boundary may be located by repeating the operation in Step 2 for each point.

### CALCULATIONAL PROCEDURE - HYPERSONIC EXTERNAL FLOW

#### CONFIGURATION 1

##### Step 1

- a. For different values of  $\alpha_1$  calculate  $\nu_1$  from the following equation:

$$\nu_1 = \alpha_1 + \nu_j - \theta_N$$

$\nu_j$  is obtained from compressible flow tables with  $M_j$  and  $\gamma_j$  for the combustion gases.  $\theta_N$  is known from the nozzle geometry.

- b. Find  $p_{b1}/p_c$  corresponding to  $\nu_1$  from the compressible flow tables for the  $\gamma$  of the exhaust gas.
- c. Plot  $p_{b1}/p_c$  versus  $\alpha_1$  from Steps a and b.
- d. For the same values of  $\alpha_1$  calculate  $p_{b1}/p_c$  using Eq. (7):

$$\frac{p_{b1}}{p_c} = \frac{p_\infty}{p_c} \left[ \gamma_\infty M_\infty^2 \sin^2 \alpha_1 + 1 \right]$$

- e. Plot  $p_{b1}/p_c$  versus  $\alpha_1$  from Step d on the same curve as Step c.
- f. From the intersection of the two curves read the values of  $\alpha_1$  and  $p_{b1}/p_c$ .
- g. Locate Point 2 by assuming one-dimensional flow from the nozzle lip, Point 1, to some arbitrary Point 2 where

$$\frac{r_2}{r_j} = 1 + \frac{\Delta r}{r_j}$$

$$\frac{x_2}{r_j} = \frac{\Delta x}{r_j} = \frac{\Delta r \cot \alpha_1}{r_j}$$

Step 2

- a. To locate Point 3, find the average internal flow conditions between Points 1 and 2 and equate this flow with the external flow as defined by Eq. (7). The calculations to determine the internal flow conditions are as follows:

1. Find  $(A/A^*)_1$  corresponding to  $p_{b1}/p_c$  from the compressible flow tables representing the exhaust gas.
2. Calculate  $(A/A^*)_2$  from

$$\left(\frac{A}{A^*}\right)_1 = \left(\frac{r_2}{r_1}\right)^2 \left(\frac{A}{A^*}\right)_2 \quad r_1 = r_j$$

3. Find  $M_{b1}$  and  $M_{b2}$  corresponding to  $(A/A^*)_1$  and  $(A/A^*)_2$ , respectively, from the compressible flow tables for the  $\gamma$  of the exhaust gas.
4. Calculate  $(M_b)_{avg}$  between Points 1 and 2 by assuming a linear Mach number distribution over the finite distance between 1 and 2

$$(M_b)_{avg} = \frac{M_{b1} + M_{b2}}{2}$$

5. Find  $(p_b/p_c)_{avg}$  corresponding to  $(M_b)_{avg}$  from the compressible flow tables representing the exhaust gas.

- b. For the internal flow, assume different values of  $\alpha_2$  and calculate  $p_{b2}/p_c$  using Eq. (4):

$$\frac{p_{b2}}{p_c} = \frac{(p_b)_{avg}}{p_c} \left[ \gamma_j (M_b)_{avg}^2 \sin^2 (\alpha_1 - \alpha_2) + 1 \right]$$

- c. Plot  $p_{b2}/p_c$  versus  $\alpha_2$  from Step 1d on the same curve as defined by the external impact equation in Step 1c.
- d. From the intersection of the two curves read the values of  $\alpha_2$  and  $p_{b2}/p_c$ .
- e. With  $\alpha_2$  determined, Point 3 may be located by assuming one-dimensional flow from Points 2 and 3 (same operation as in Step 1g using Eqs. (2) and (3)).

Subsequent points along the boundary may be located by repeating the operation in Step 2 for each point.

## CONFIGURATION 2

### Step 1

Calculate the constant pressure portion of the boundary (nozzle lip, Point 1, to the point of intersection with the free stream, Point i) as outlined for the quiescent atmosphere.

### Step 2

a. Determine the internal flow conditions prior to interaction with the free stream as follows: (Note:  $n = i - 1$ .)

1. Find  $(A/A^*)_{i-1}$  corresponding to  $p_{b_{i-1}}/p_c$  from the compressible flow tables representing the exhaust gas.
2. Calculate  $(A/A^*)_i$  from

$$\left(\frac{A}{A^*}\right)_i = \frac{(r_i)^2}{(r_{i-1})^2} \left(\frac{A}{A^*}\right)_{i-1}$$

3. Find  $M_{b_{i-1}}$  and  $M_{b_i}$  corresponding to  $(A/A^*)_{i-1}$  and  $(A/A^*)_i$ , respectively, from the compressible flow tables for the  $\gamma$  of the exhaust gas.
4. Calculate  $(M_b)_{avg}$  between  $(i-1)$  and  $(i)$  by assuming a linear Mach number distribution over the finite distance between  $(i-1)$  and  $(i)$ :

$$(M_b)_{avg} = \frac{(M_b)_{i-1} + (M_b)_i}{2}$$

5. Find  $(p_b/p_c)_{avg}$  corresponding to  $(M_b)_{avg}$  from the compressible flow tables representing  $\gamma_j$ .
- b. With the average internal flow conditions between  $(i-1)$  and  $(i)$  defined, the calculations for the boundary are the same as for Configuration 1, Steps 2b-2e.

## CALCULATIONAL PROCEDURE - SUPERSONIC EXTERNAL FLOW

### CONFIGURATION 1

#### Step 1

a. For different values of  $\alpha_1$  calculate  $\nu_1$  from the following equation:

$$\nu_1 = \nu_1 + \nu_j \theta_N$$

$\nu_j$  is obtained from compressible flow tables with  $M_j$  and  $\gamma_j$  for the exhaust gas.  $\theta_N$  is known from the nozzle geometry.

- b. Find  $p_{b1}/p_c$  corresponding to  $\nu_1$  from the compressible flow tables for the  $\gamma$  of the exhaust gas.
- c. Plot  $p_{b1}/p_c$  versus  $\alpha_1$  from Steps a and b.
- d. For the same values of  $\alpha_1$ , find the corresponding pressure coefficient  $C_p$  from conical flow charts based on  $\gamma_\infty$ . The pressure coefficient is defined as

$$C_p = \frac{p_{b1} - p_\infty}{q_\infty} = \frac{2}{\gamma_\infty M_\infty^2} \left[ \frac{p_{b1}}{p_\infty} - 1 \right]$$

where  $C_p = f(\alpha_1, M_\infty)$ .

- e. Solve for  $p_{b1}/p_c$  as follows:

$$\frac{p_{b1}}{p_c} = \frac{p_\infty}{p_c} \left[ \frac{\gamma_\infty M_\infty^2 C_p}{2} + 1 \right]$$

$\gamma_\infty$ ,  $M_\infty$ , and  $p_\infty$  are known from the external flow conditions.

- f. Plot  $p_{b1}/p_c$  versus  $\alpha_1$ , from Steps d and e on the same curve as Step c.
- g. From the intersection of the two curves read the values of  $\alpha_1$  and  $p_{b1}/p_c$ .
- h. Locate Point 2 by assuming one-dimensional flow from the nozzle lip, Point 1, to some arbitrary Point 2 where

$$\frac{r_2}{r_j} = 1 + \frac{\Delta r}{r_j}$$

$$\frac{x_2}{r_j} = \frac{\Delta x}{r_j} = \frac{\Delta r \cot \alpha_1}{r_j}$$

## Step 2

Successive points are established by finding an estimated average flow between two preceding points and predicting the pressure at the end of the interval by Newtonian impact theory. Equilibrium is sought with the external flow which is assumed to be governed by Prandtl-Meyer expansion of the external flow behind the conical shock referred to in Step 1.

- a. Define the external flow aft of the external shock as follows:
  1. Find the external Mach number,  $M_{\omega 1}$ , behind the external shock corresponding to  $M_\infty$  and  $\alpha_1$  from conical flow tables.

2. From compressible flow tables based on  $\gamma_\infty$ , find  $\nu_{\infty 1}$  corresponding to  $M_{\infty 1}$ .
- b. For different values of  $\alpha_2$ , calculate  $\nu_{\infty 2}$  as follows:

$$\nu_{\infty 2} = \nu_{\infty 1} + (\alpha_1 - \alpha_2)$$

- c. Find  $p_{b2}/p_t$  corresponding to  $\nu_{\infty 2}$  from compressible flow tables.  $p_t$  is the stagnation pressure of the external flow behind the conical shock.
- d. Calculate  $p_{b2}/p_c$  as follows:

$$\frac{p_{b2}}{p_c} = \frac{p_{b2}}{p_t} \left( \frac{p_{b1}}{p_c} \right) \left( \frac{p_t}{p_{b1}} \right)$$

$p_{b1}/p_c$  is obtained from Step 1g and  $p_t/p_{b1}$  corresponds to  $\nu_{\infty 1}$  in Step 2b.

- e. Plot  $p_{b2}/p_c$  versus  $\alpha_2$  from Steps 2b and 2d.

The computations of the internal flow for the step-by-step equilibrium of internal and external pressures to determine the jet boundary is outlined in the following steps to determine Point 3.

- f. Calculate the average flow conditions between Points 1 and 2 as follows:
1. Find  $(A/A^*)_2$  corresponding to  $p_{b1}/p_c$  from the compressible flow tables representing the exhaust gas.
  2. Calculate  $(A/A^*)_2$  from

$$\left( \frac{A}{A^*} \right)_1 = \left( \frac{r_2}{r_1} \right)^2 \left( \frac{A}{A^*} \right)_2 \quad r_1 = r_j$$

3. Find  $M_{b1}$  and  $M_{b2}$  corresponding to  $(A/A^*)_1$  and  $(A/A^*)_2$ , respectively, from the compressible flow tables for the  $\gamma$  of the exhaust gas.
4. Calculate  $(M_b)_{avg}$  between Points 1 and 2 by assuming a linear Mach number distribution over the finite distance between 1 and 2.

$$(M_b)_{avg} = \frac{M_{b1} + M_{b2}}{2}$$

5. Find  $(p_b/p_c)_{avg}$  corresponding to  $(M_b)_{avg}$  from the compressible flow tables representing the exhaust gas.

- g. For the internal flow, assume different values of  $\alpha_2$  and calculate  $p_{b2}/p_c$  using Eq. (4):

$$\frac{p_{b2}}{p_c} = \frac{(p_b)_{avg}}{p_c} \left[ \gamma_j (M_b)_{avg}^2 \sin^2 (\alpha_1 - \alpha_2) + 1 \right]$$

- h. Plot  $p_{b2}/p_c$  versus  $\alpha_2$  from Step d on the same curve as defined by the external impact equation in Step 2e.
- i. From the intersection of the two curves read the values of  $\alpha_2$  and  $p_{b2}/p_c$ .
- j. With  $\alpha_2$  determined, Point 3 may be located by assuming one-dimensional flow from 2 to 3 (same operation as in Step 1h using Eqs. (2) and (3)).

Subsequent points along the boundary may be located by repeating the operation in Step 2 for each point.

## CONFIGURATION 2

### Step 1

Calculate the constant pressure portion of the boundary (nozzle lip, Point 1, to the point of intersection with the free stream, Point i) as outlined for the quiescent atmosphere.

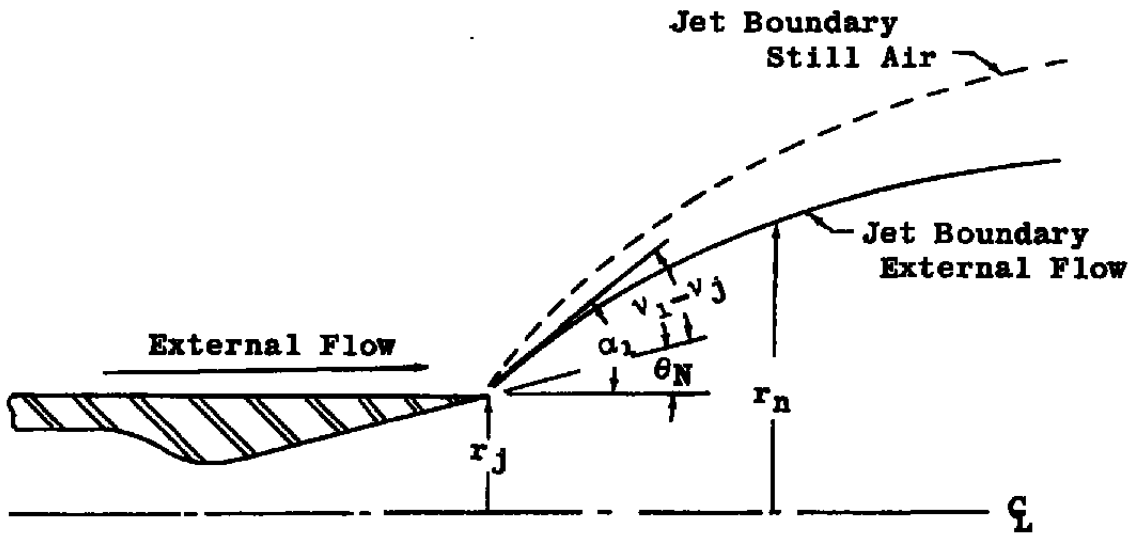
### Step 2

- a. Determine the internal flow conditions prior to interaction with the free stream as follows: (Note:  $n = i - 1$ .)
1. Find  $(A/A^*)_{i-1}$  corresponding to  $p_{b_{i-1}}/p_c$  from the compressible flow tables representing the exhaust gas.
  2. Calculate  $(A/A^*)_i$  from
 
$$\left(\frac{A}{A^*}\right)_i = \frac{(r_i)^2}{(r_{i-1})^2} \left(\frac{A}{A^*}\right)_{i-1}$$
  3. Find  $M_{b_{i-1}}$  and  $M_{b_i}$  corresponding to  $(A/A^*)_{i-1}$  and  $(A/A^*)_i$ , respectively, from the compressible flow tables for the  $\gamma$  of the exhaust gas.
  4. Calculate  $(M_b)_{avg}$  between  $(i-1)$  and  $(i)$  by assuming a linear Mach number distribution over the finite distance between  $(i-1)$  and  $(i)$ :

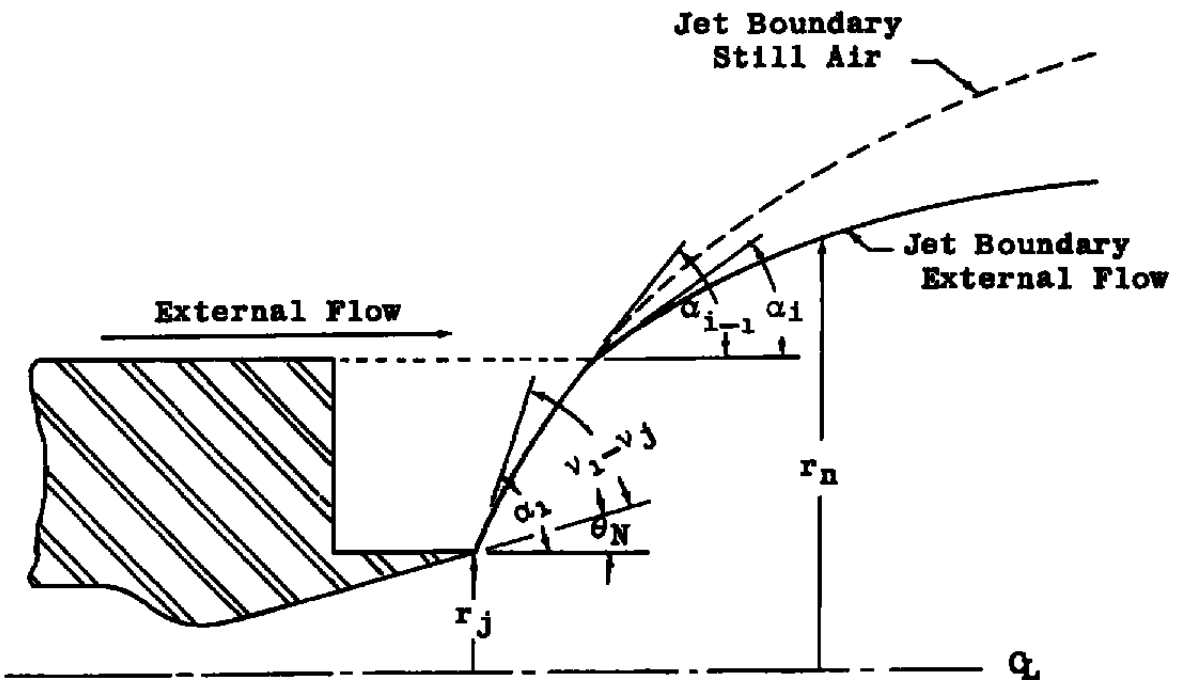
$$(M_b)_{avg} = \frac{(M_b)_{i-1} + M_{b_i}}{2}$$

5. Find  $(p_b/p_c)_{avg}$  corresponding to  $(M_b)_{avg}$  from the compressible flow tables representing  $\gamma_j$ .
- b. Assume different values of  $\alpha_i$  and calculate  $p_{b_i}/p_c$  using Eq. (4):
- $$\frac{p_{b_i}}{p_c} = \frac{(p_b)_{avg}}{p_c} \left[ \gamma_j (M_b)_{avg}^2 \sin^2 (\alpha_{i-1} - \alpha_i) + 1 \right]$$
- c. Plot  $p_{b_i}/p_c$  versus  $\alpha_i$  from Step 2b.
- d. For the same values of  $\alpha_i$ , find  $p_{b_i}/p_c$  for the external flow from Steps 1d and 1e for Configuration 1.
- e. Plot  $p_{b_i}/p_c$  versus  $\alpha_i$  from Step 2c on the same curve as Step 2d.
- f. From the intersection of the two curves read the values of  $\alpha_i$  and  $p_{b_i}/p_c$ .
- g. Locate Point (i+1) as in Step 1h for Configuration 1.

Successive points are obtained by repeating the operations outlined in Step 2 for Configuration 1.



a. Configuration 1



h. Configuration 2

Fig. 1 Schematic of Model Configurations

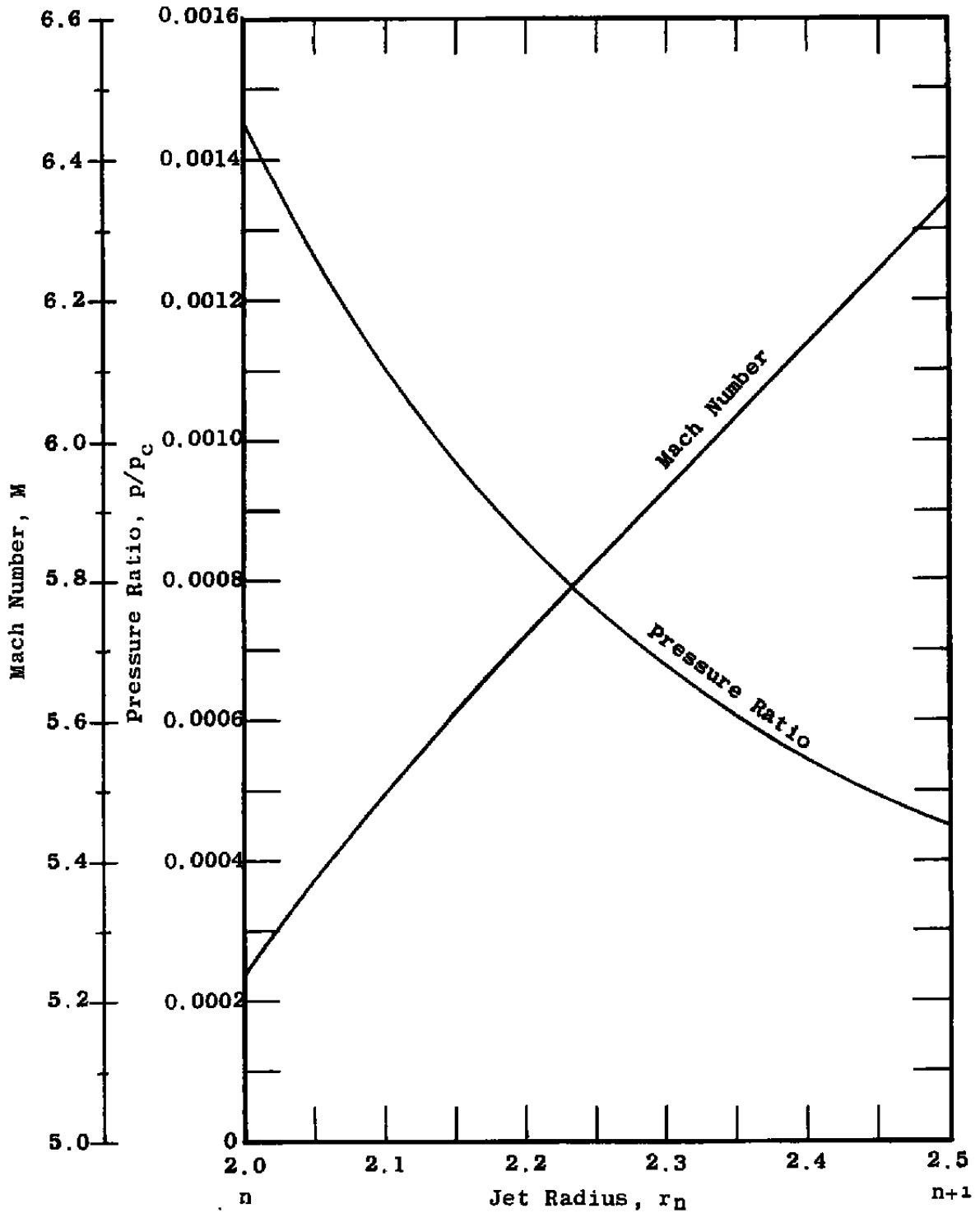


Fig. 2 Pressure Ratio and Mach Number versus Jet Radius between Two Points on a Boundary,  $(n)$  and  $(n+1)$

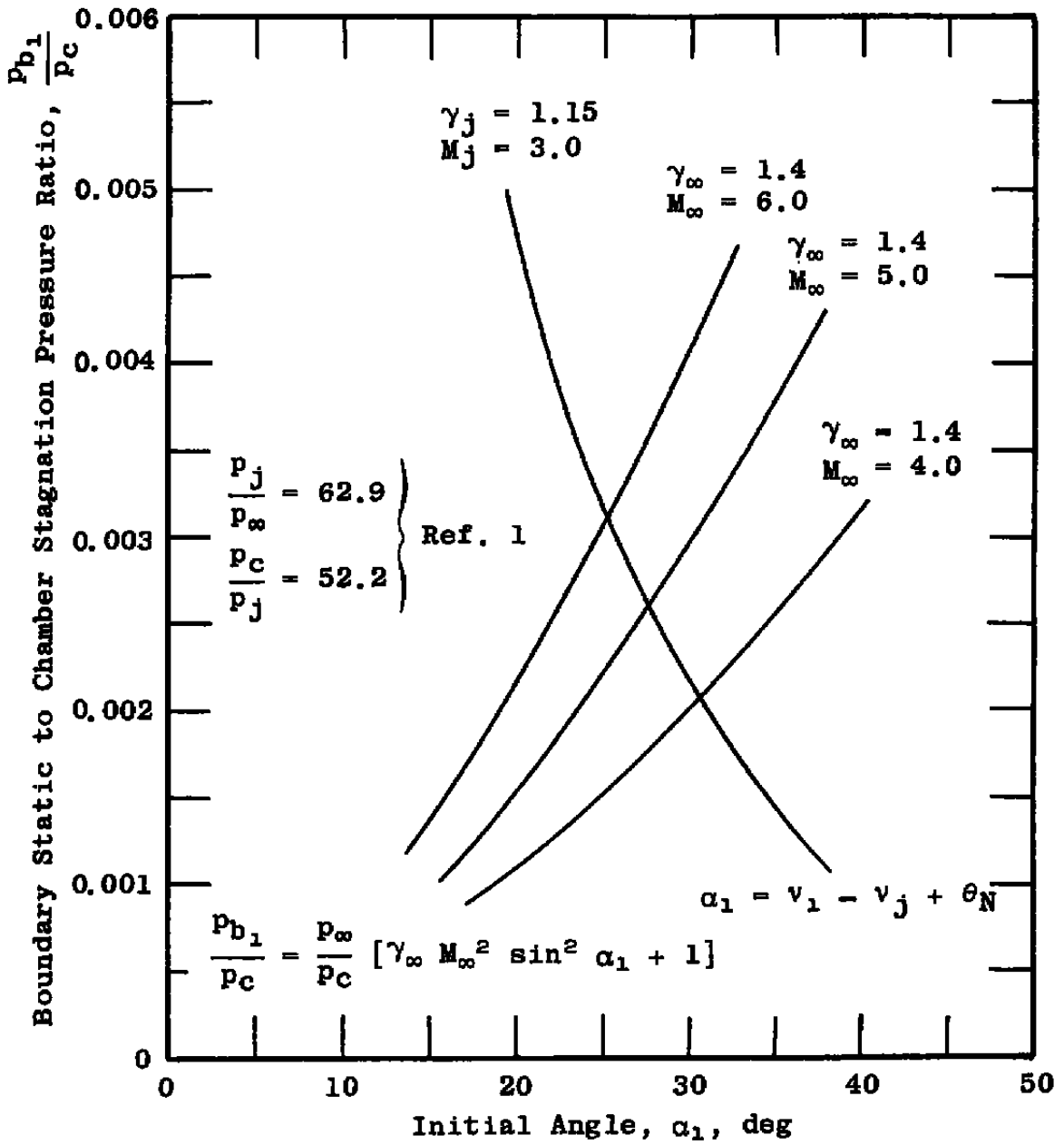
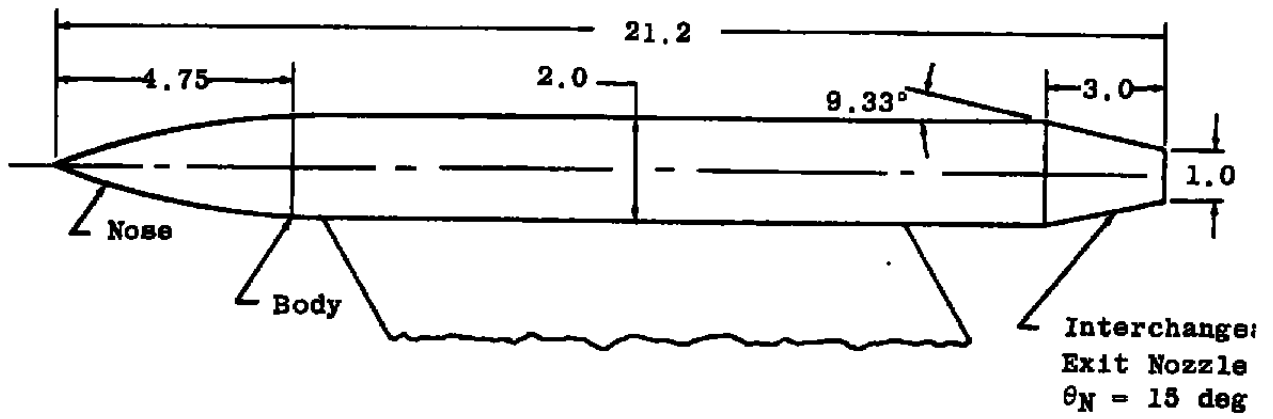
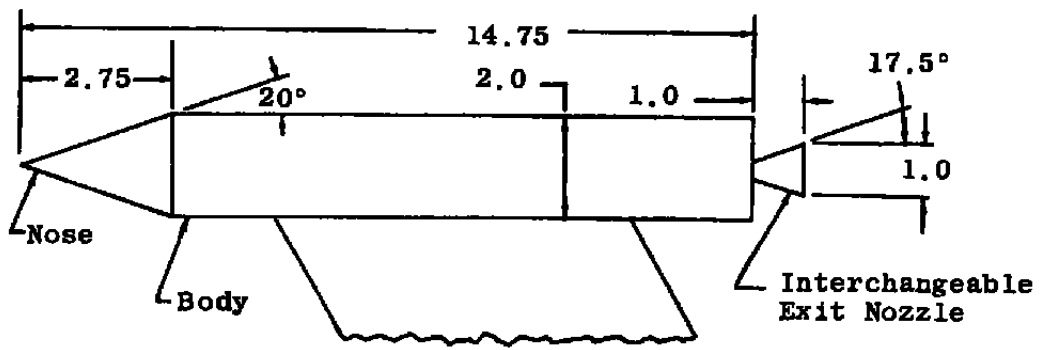


Fig. 3 Initial Angle Plot



a.  $D/D_i = 1.0, M_i = 2.5$



b.  $D/D_i = 2.0, M_i = 3.7$

Note: All dimensions in inches

Fig. 4 Schematic of Test Models

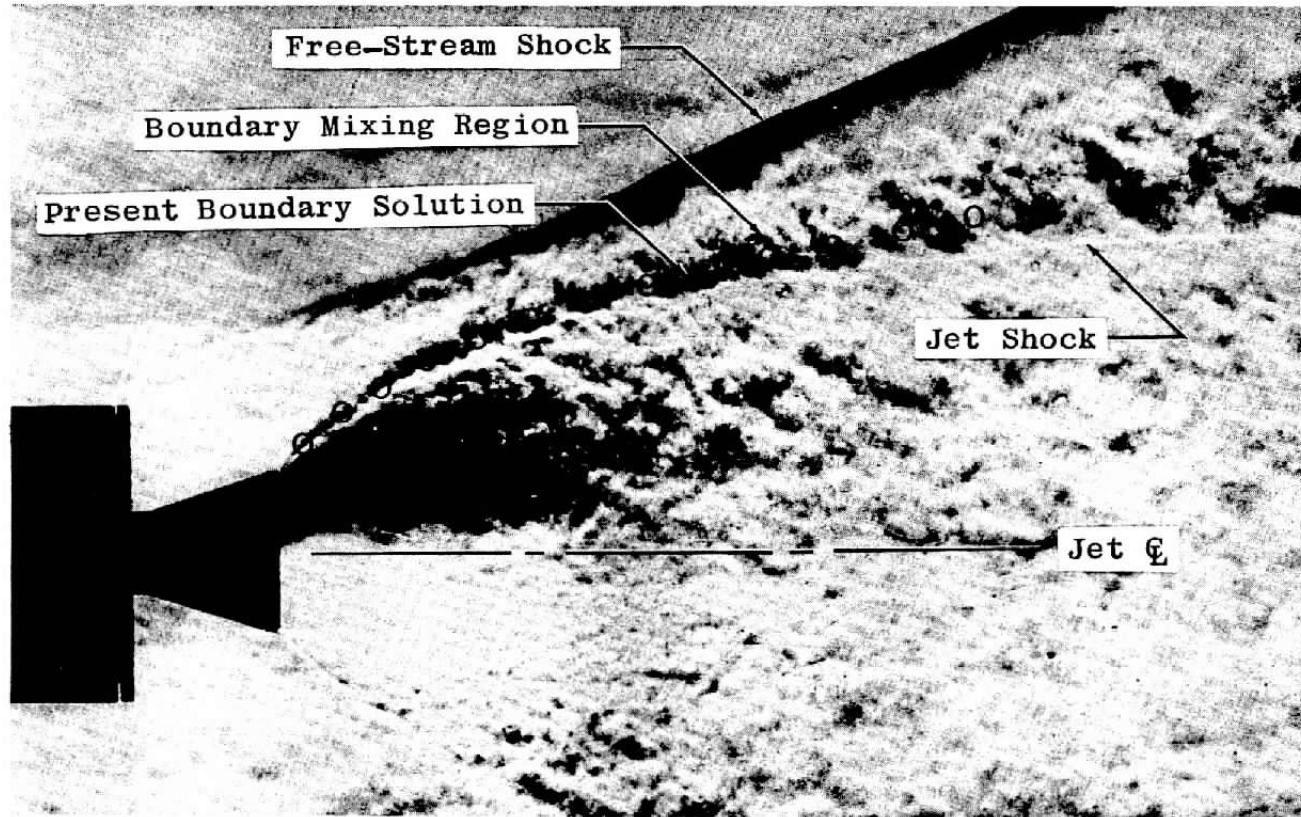


Fig. 5 Typical Schlieren Photograph of the Jet Structure,  $M_\infty = 5.0$

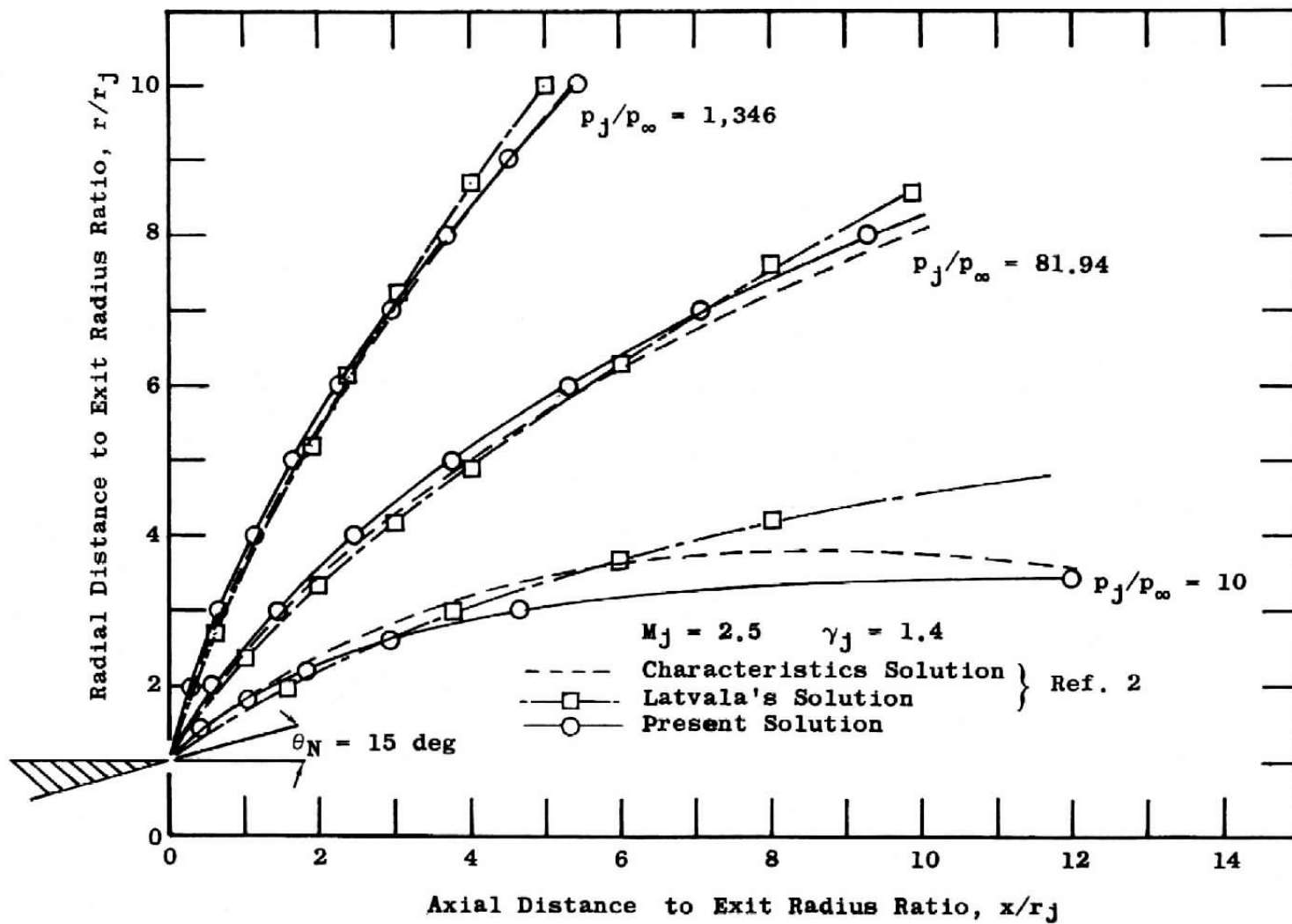
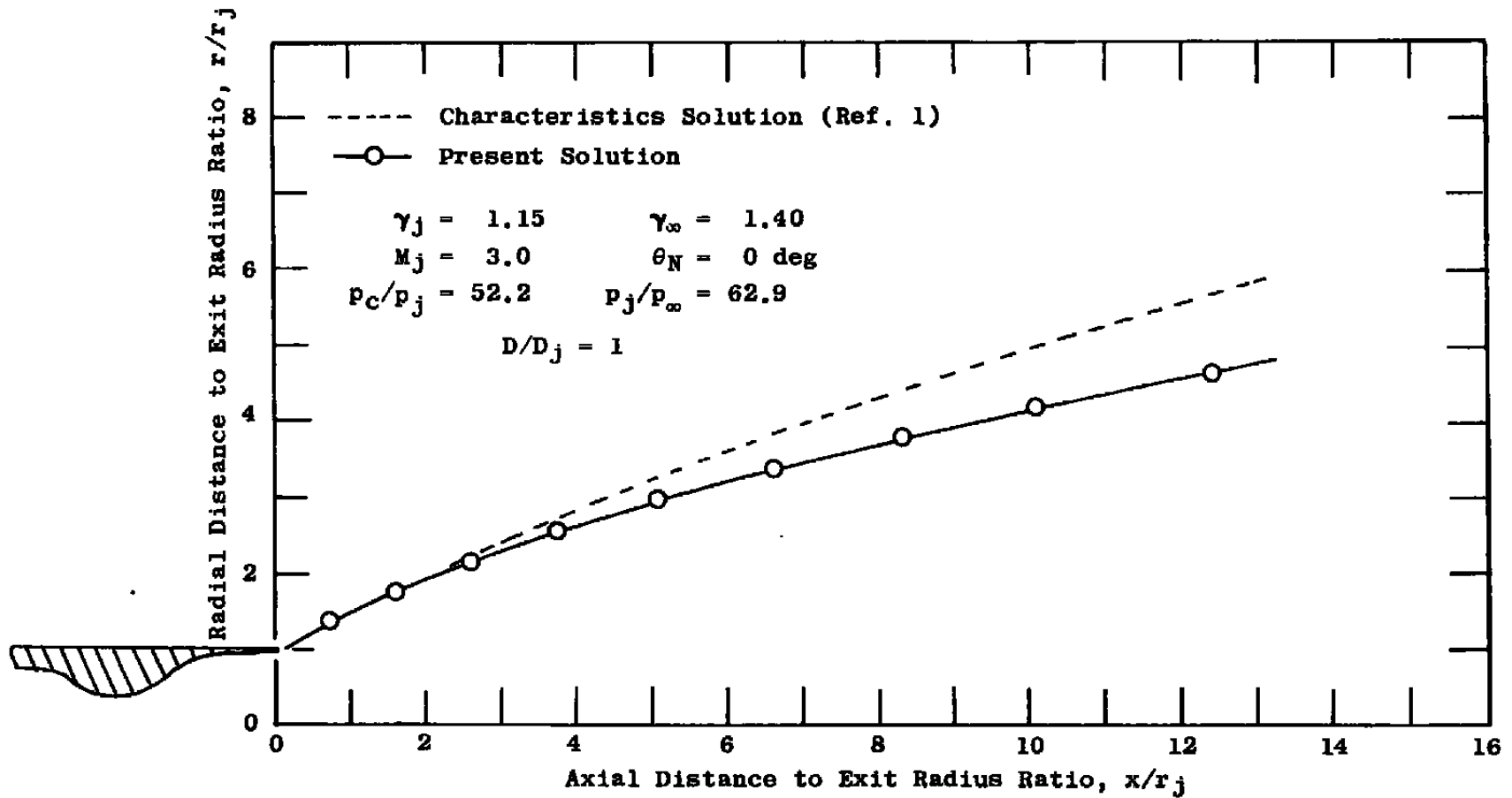
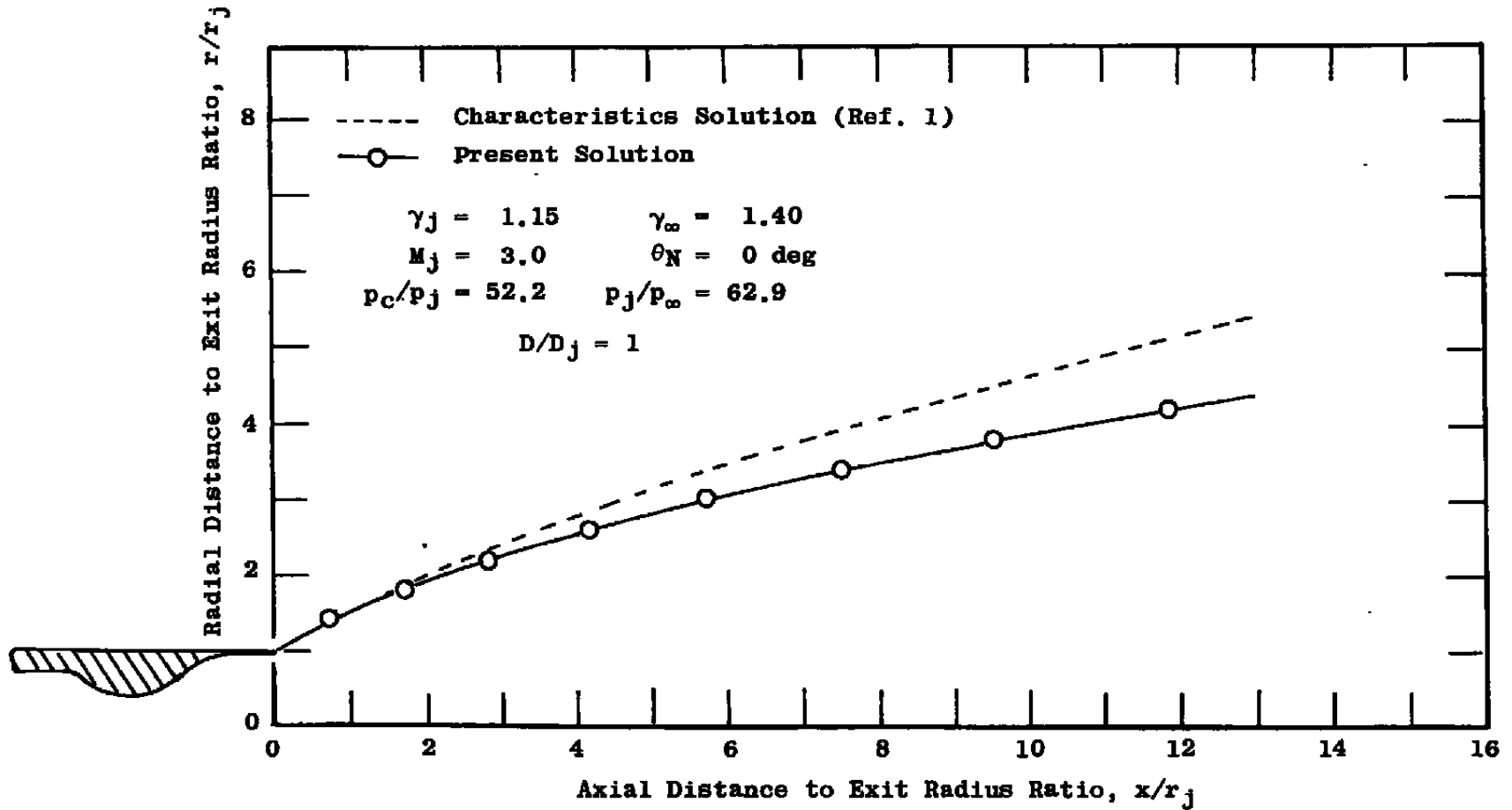


Fig. 6 Jet Boundaries Calculated by the Present Quiescent Method Compared with the Method of Characteristics Solution and Latvala's Solution for a Quiescent Atmosphere



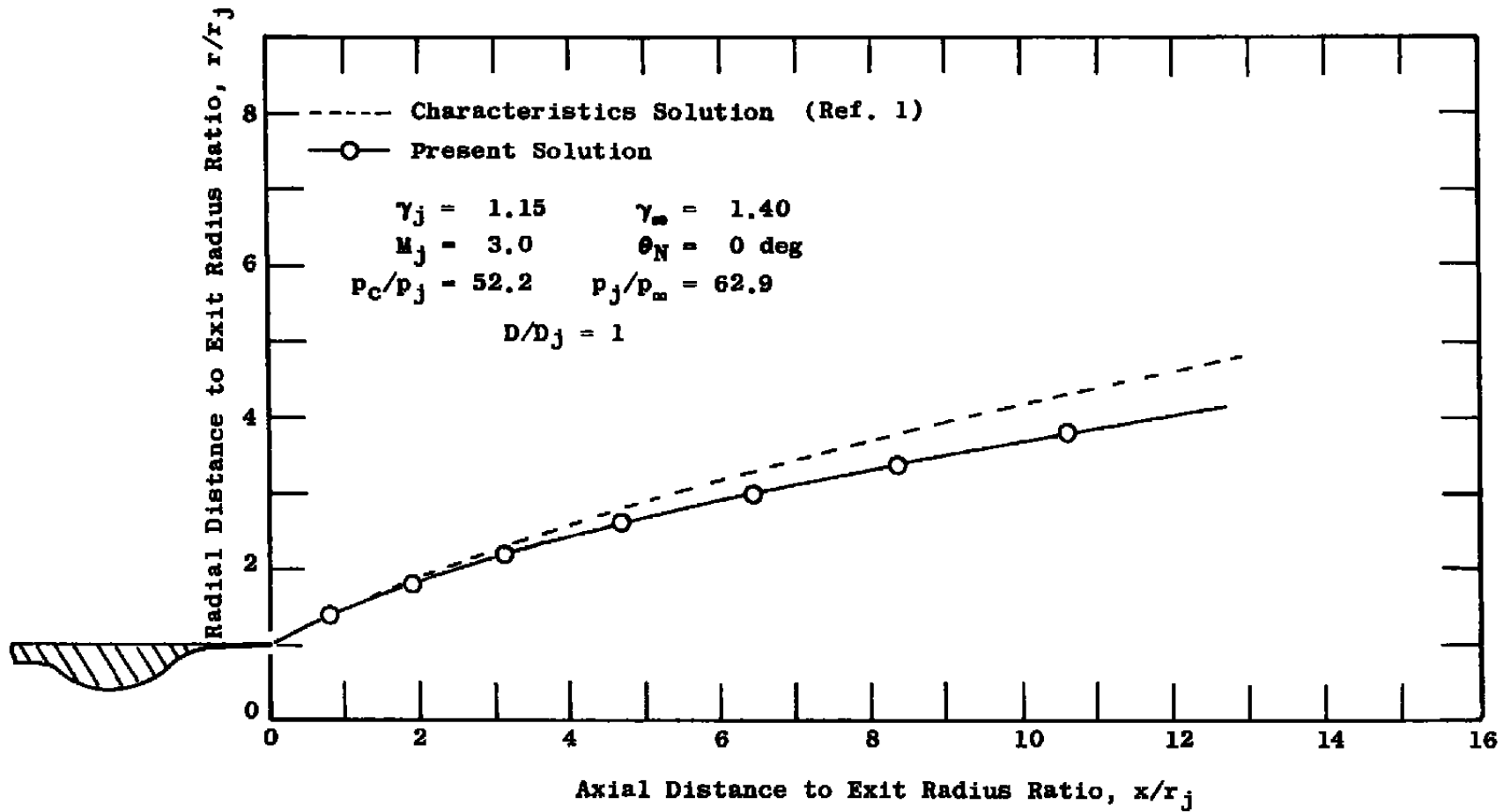
a. Boundary Comparison,  $M_\infty = 4.0$

Fig. 7 Jet Boundaries Calculated by the Present Hypersonic Method Compared with the Method of Characteristics Solution



b. Boundary Comparison,  $M_\infty = 5.0$

Fig. 7 Continued



c. Boundary Comparison,  $M_\infty = 6.0$

Fig. 7 Concluded

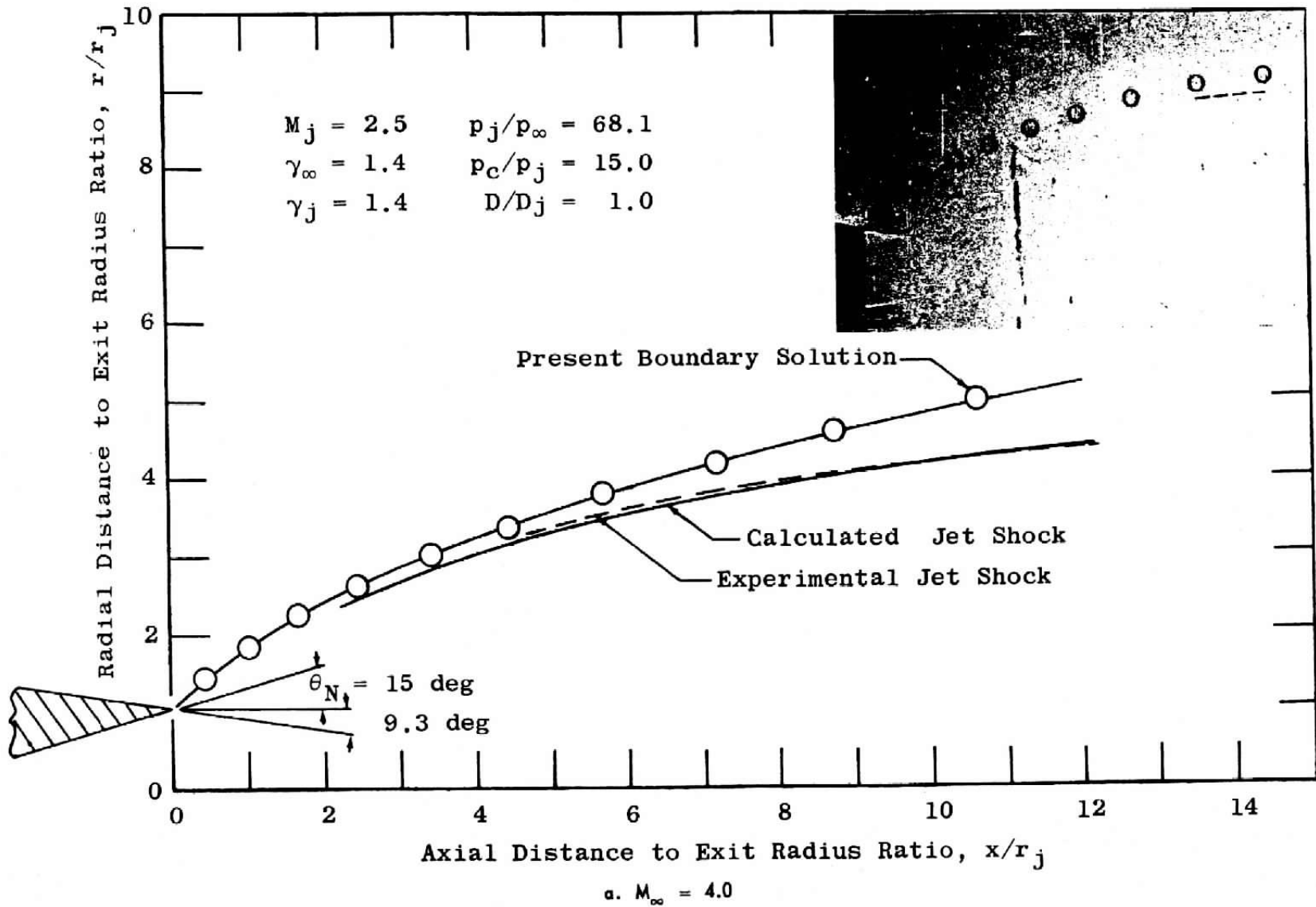
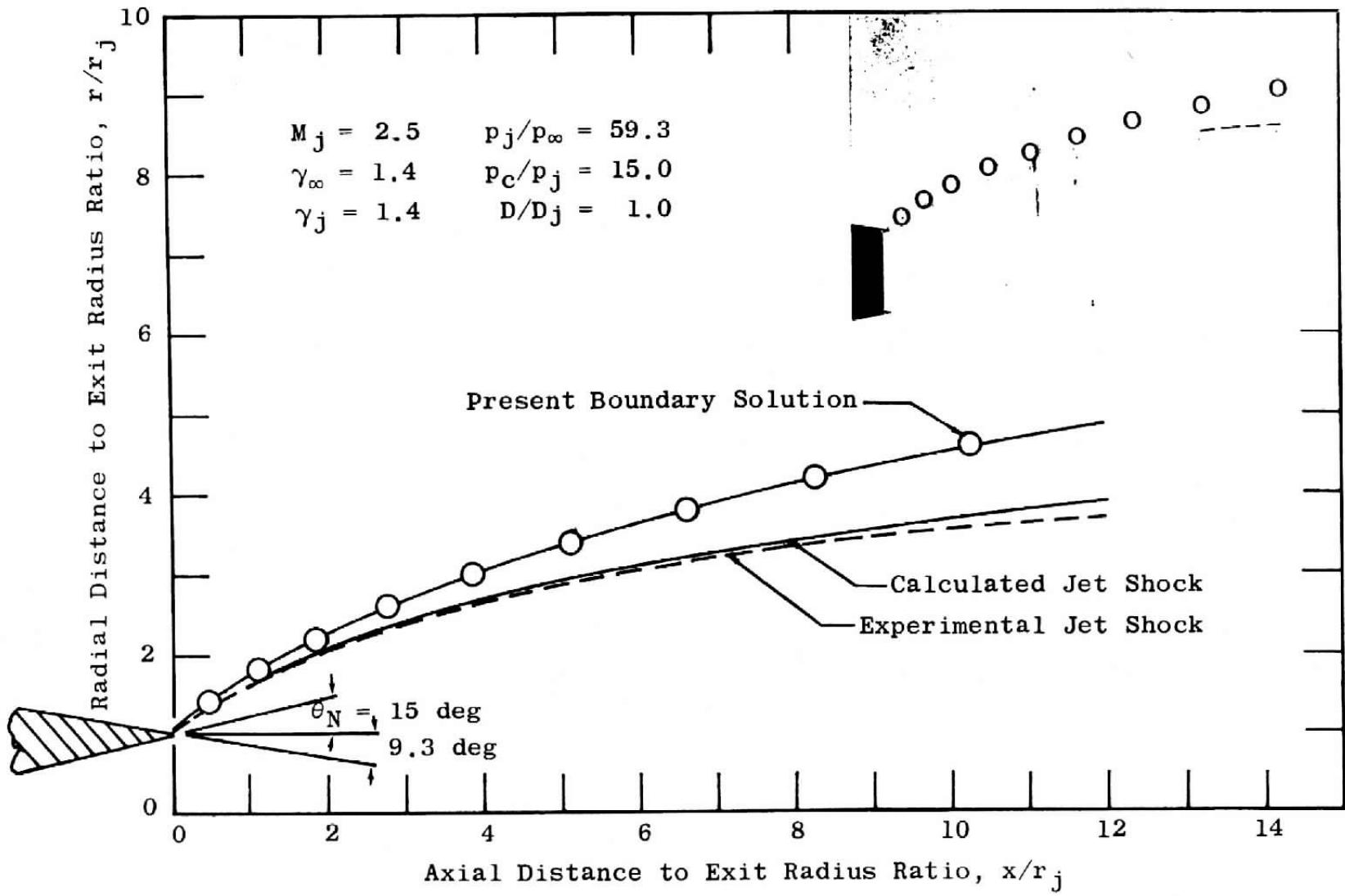


Fig. 8 Jet Boundaries Calculated by the Present Hypersonic Method Compared with Experimental Jet Shocks



b.  $M_\infty = 5.0$

Fig. 8 Concluded

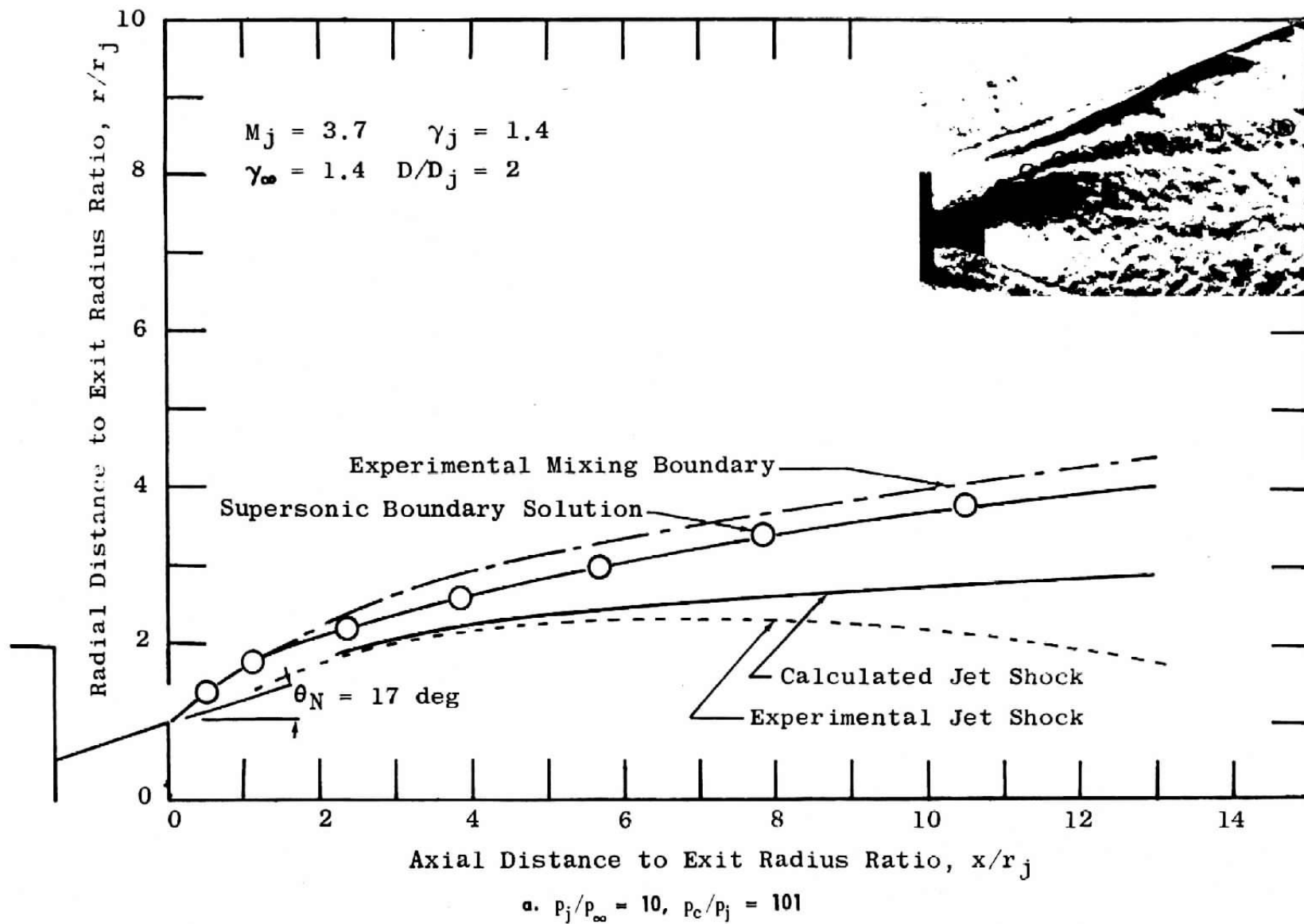
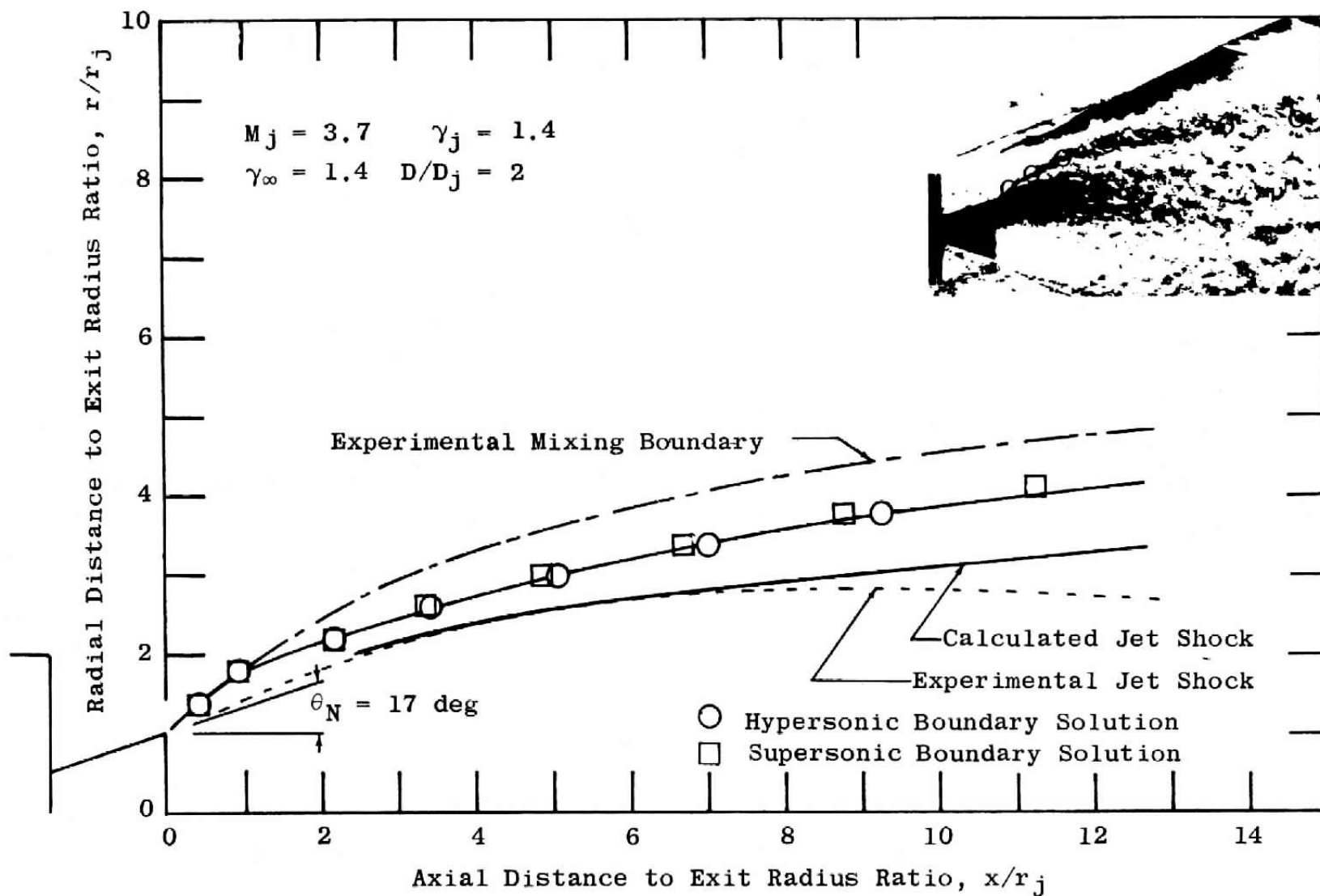


Fig. 9 Jet Boundaries Calculated by the Present Methods Compared with Experimental Boundaries,  $M_\infty = 3.5$



b.  $p_j/p_\infty = 15$ ,  $p_c/p_j = 101$

Fig. 9 Concluded

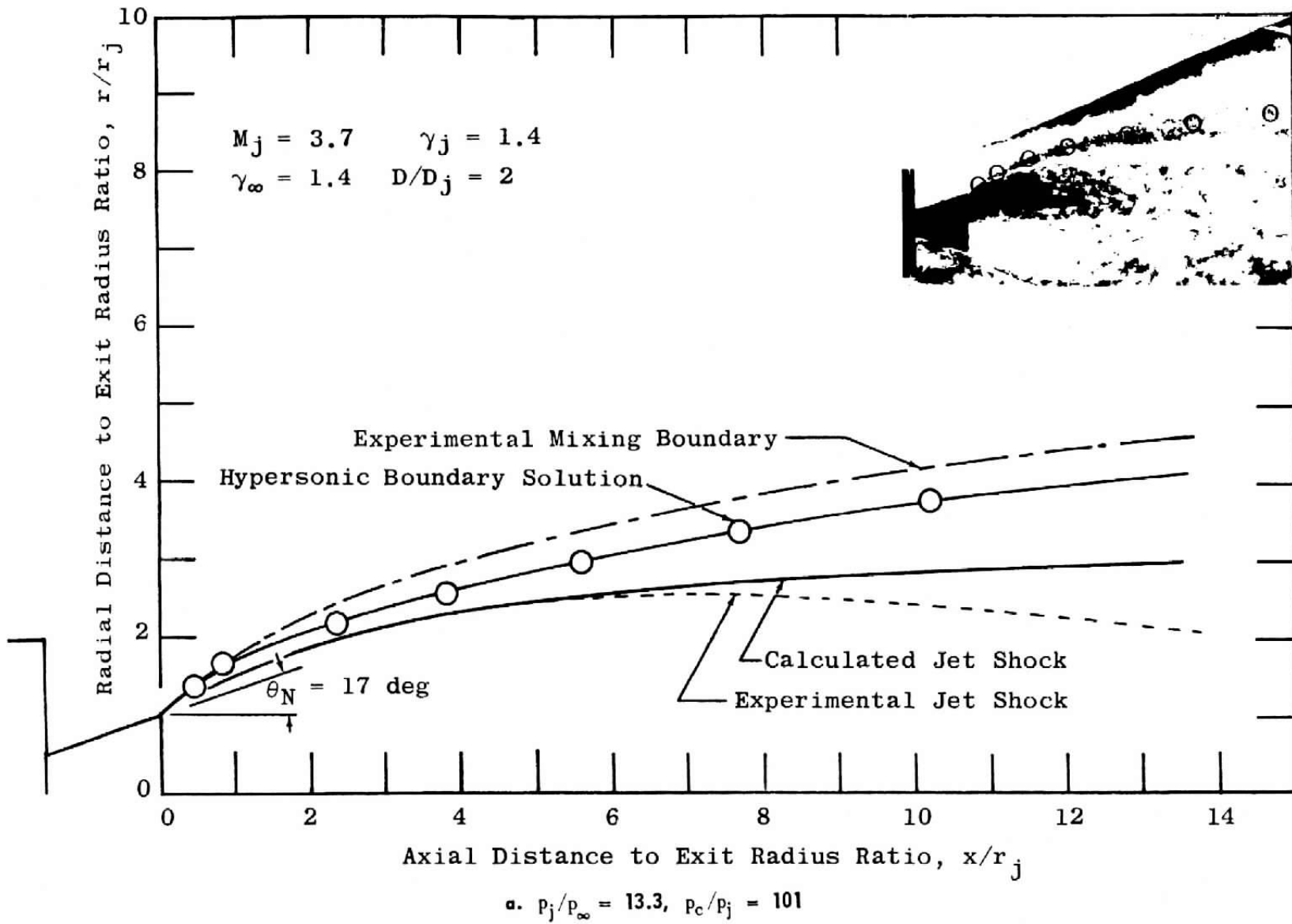
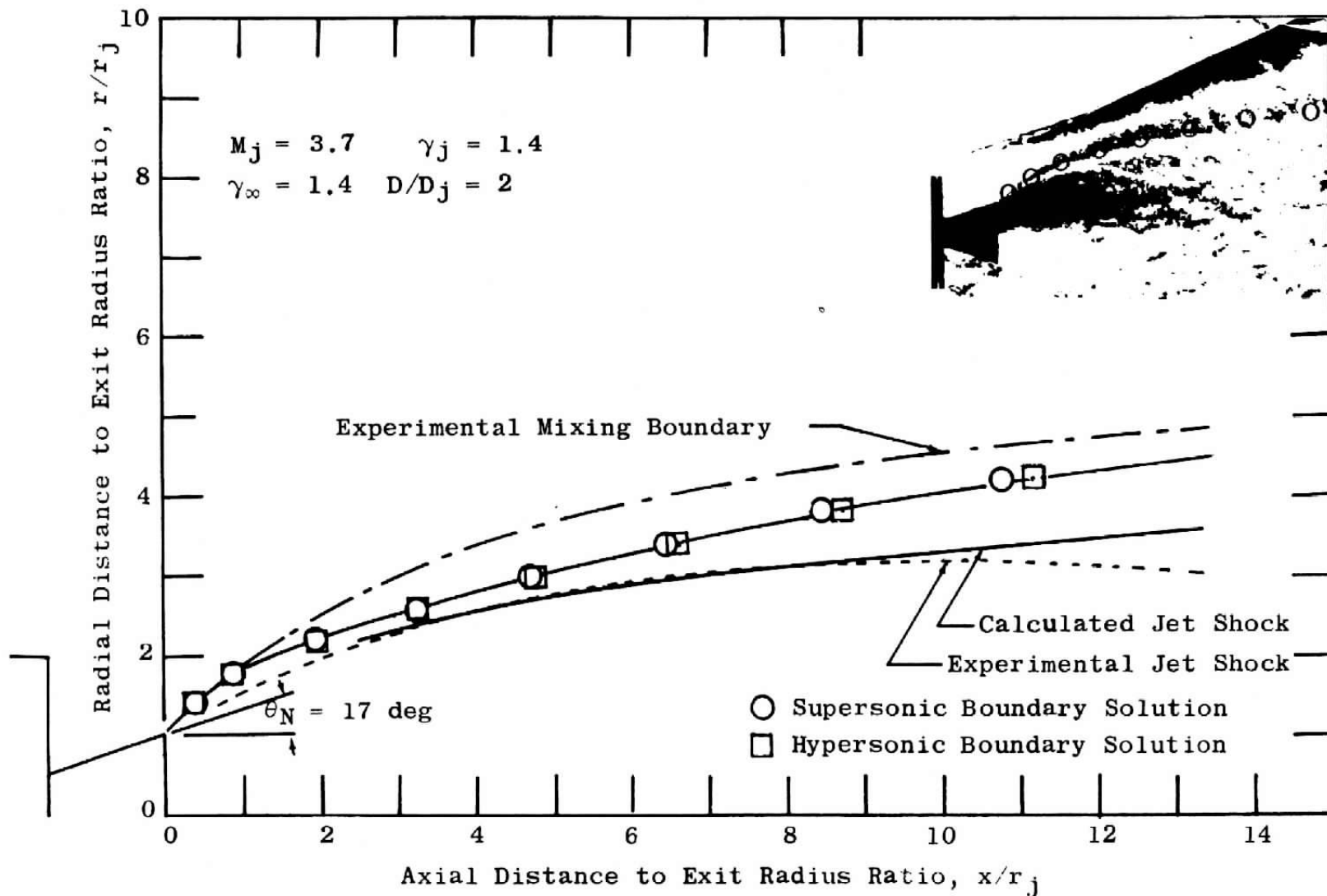


Fig. 10 Jet Boundaries Calculated by the Present Methods Compared with Experimental Boundaries,  $M = 4.0$



b.  $p_j/p_\infty = 20.0$ ,  $p_c/p_j = 101$

Fig. 10 Concluded

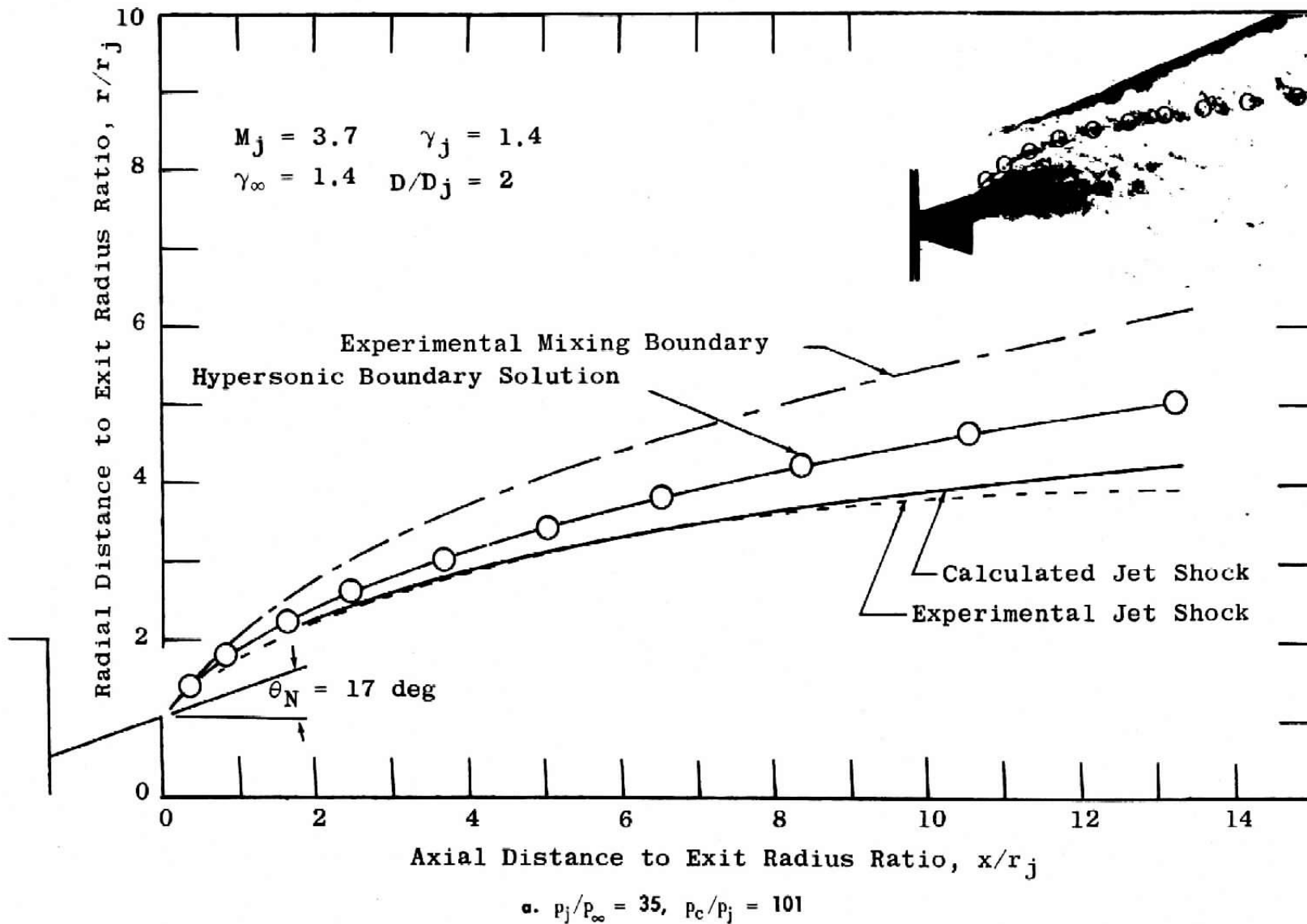
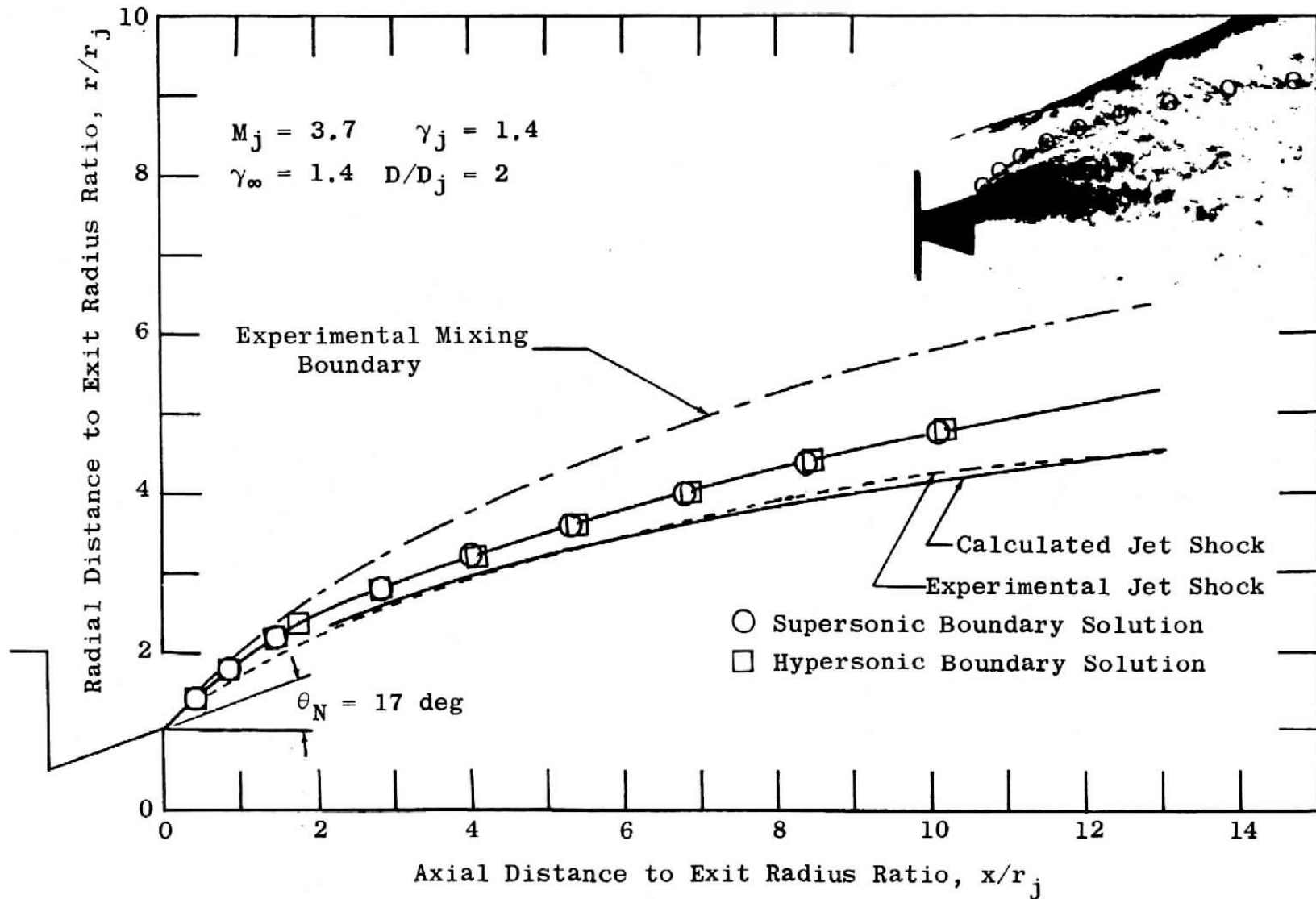


Fig. 11 Jet Boundaries Calculated by the Present Methods Compared with Experimental Boundaries,  $M_\infty = 5.0$



b.  $p_j/p_\infty = 52$ ,  $p_c/p_j = 101$

Fig. 11 Concluded

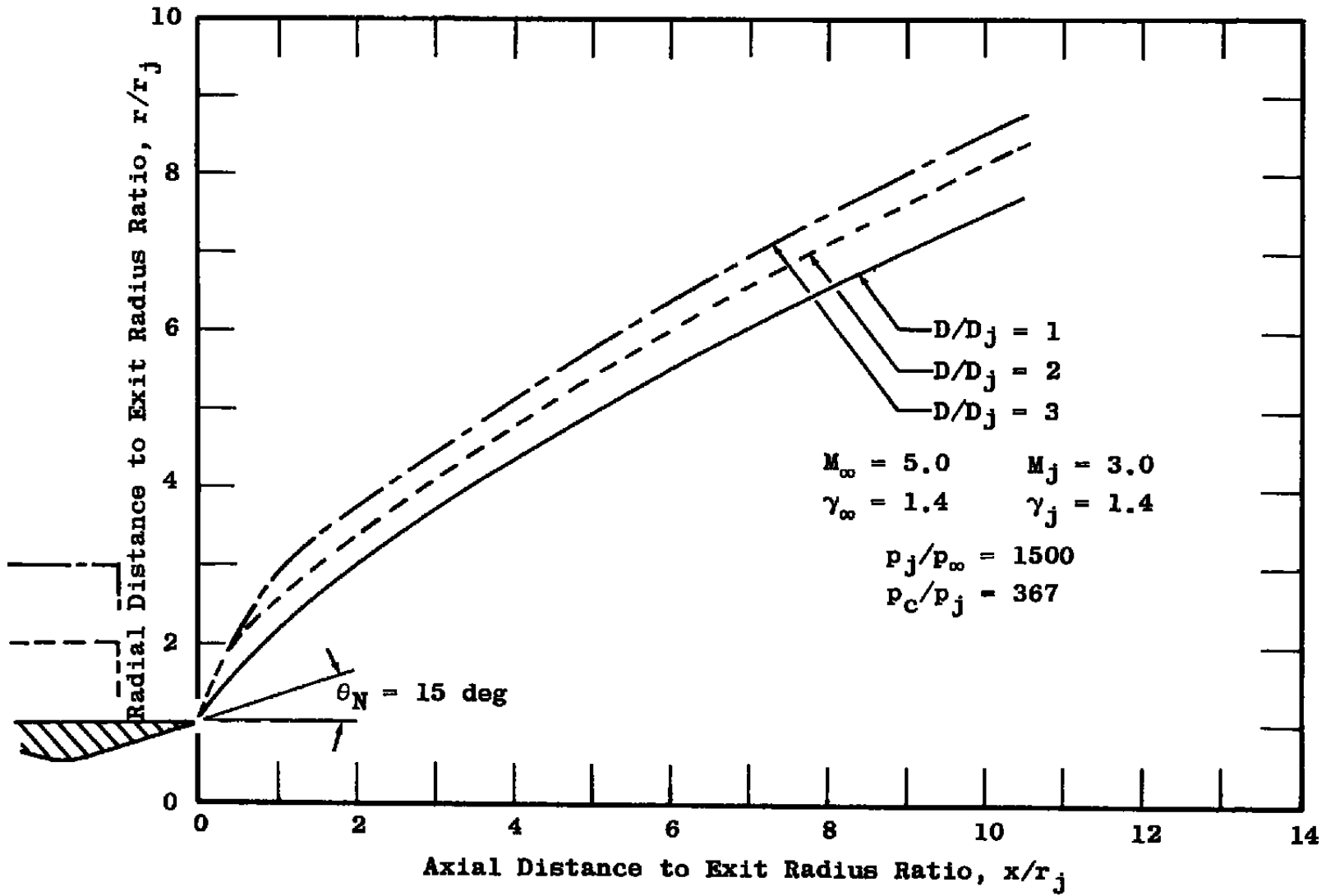
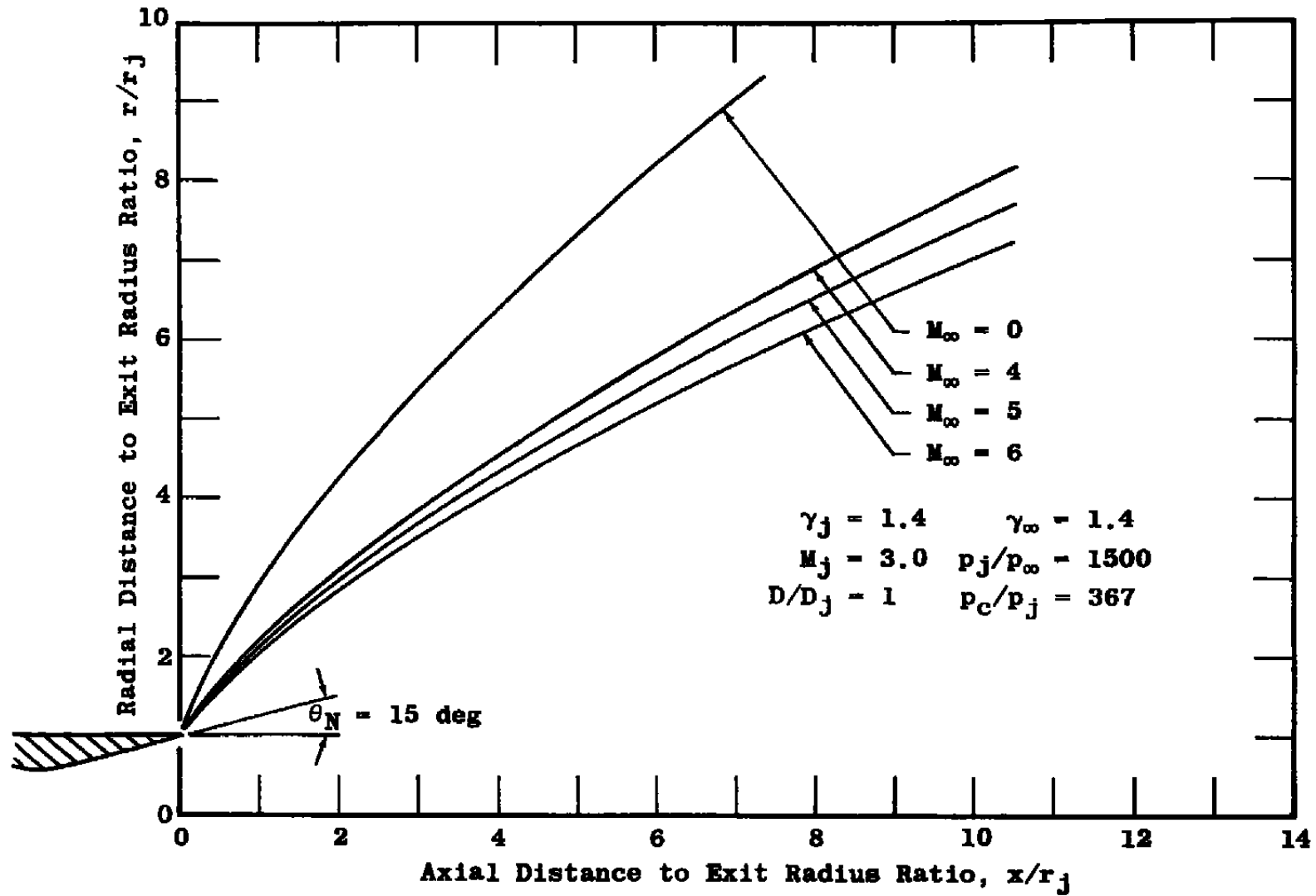
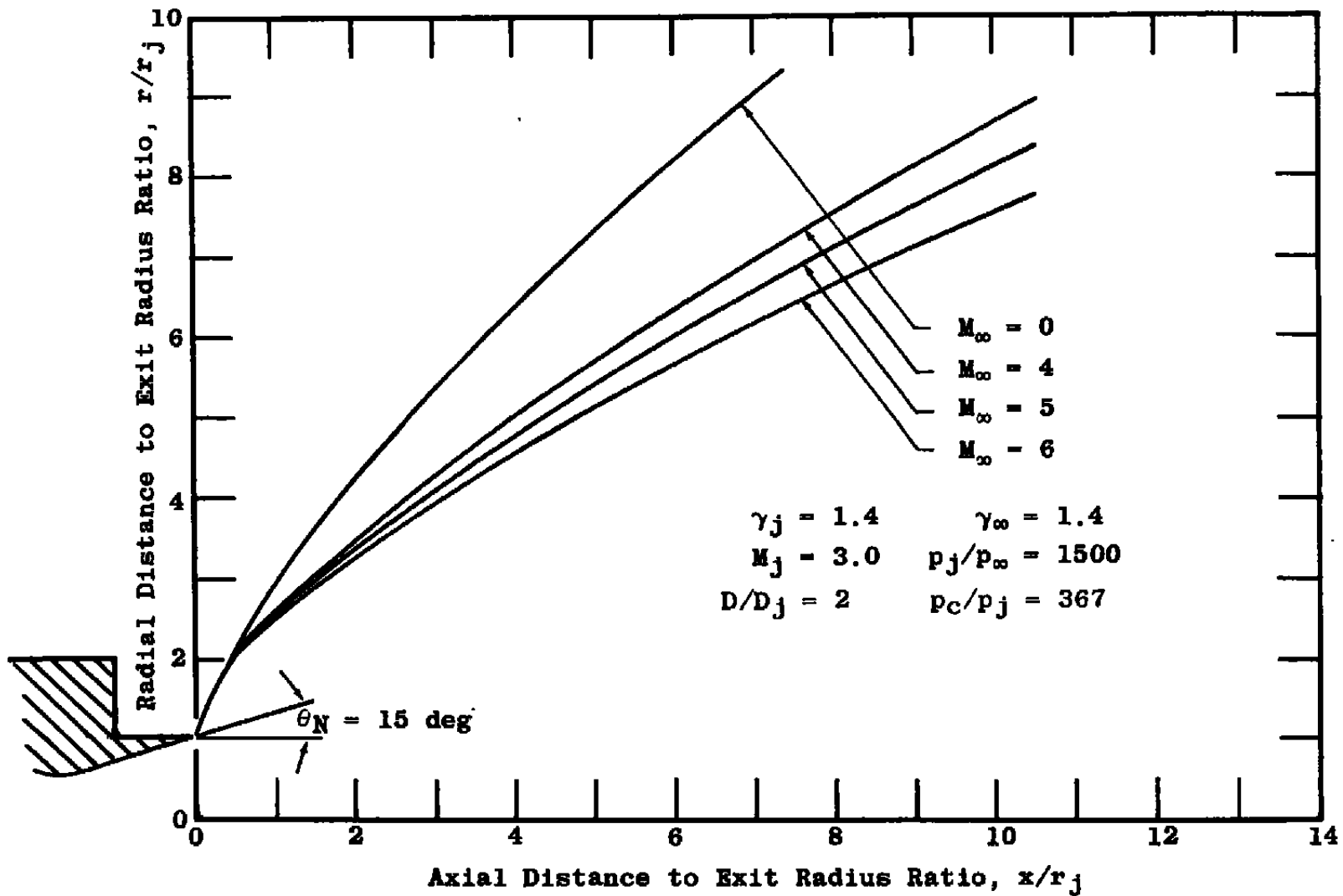


Fig. 12 Comparison of Jet Boundaries Calculated by the Present Hypersonic Method for Configurations 1 and 2



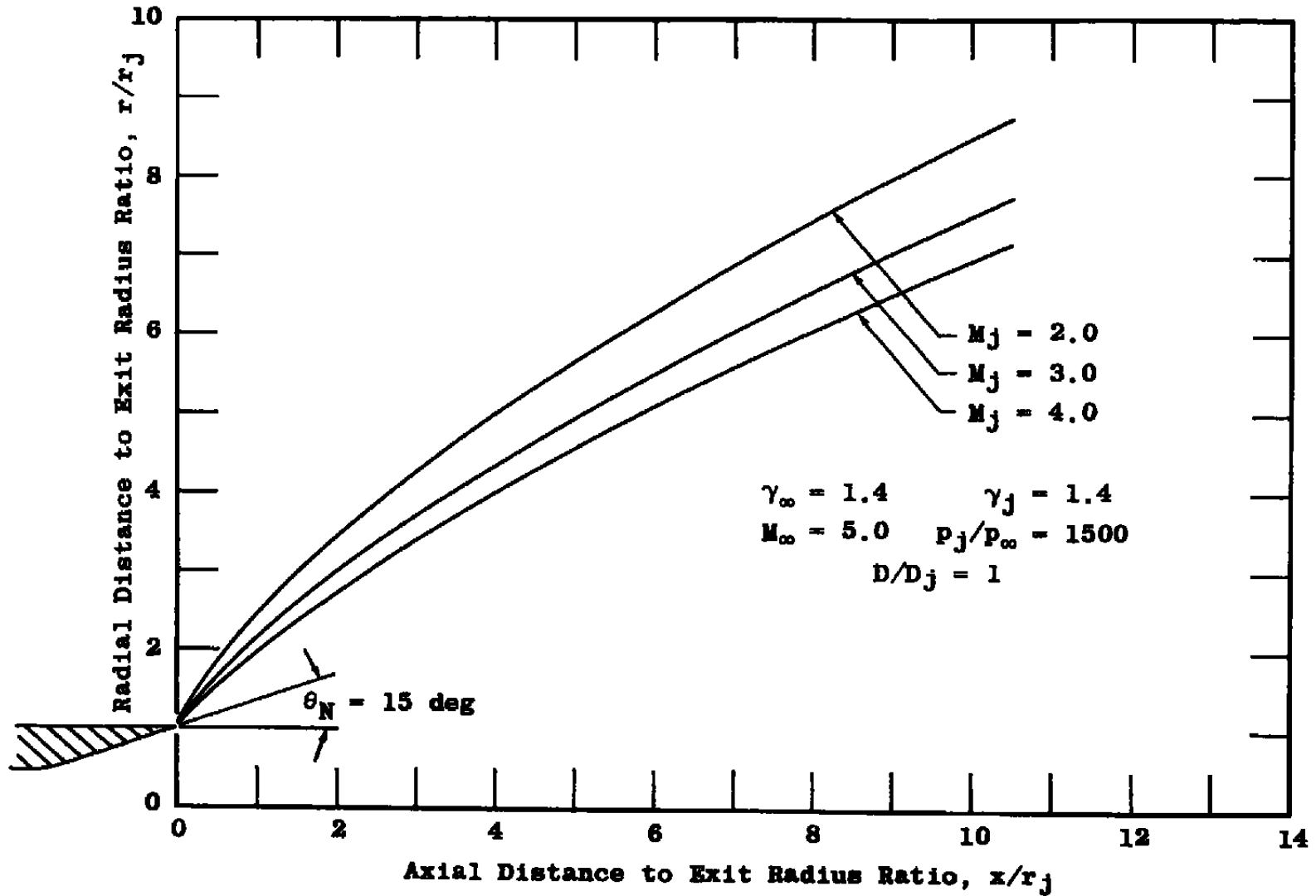
a. Configuration 1

Fig. 13 Jet Boundaries Calculated by the Present Methods for Various Free-Stream Mach Numbers



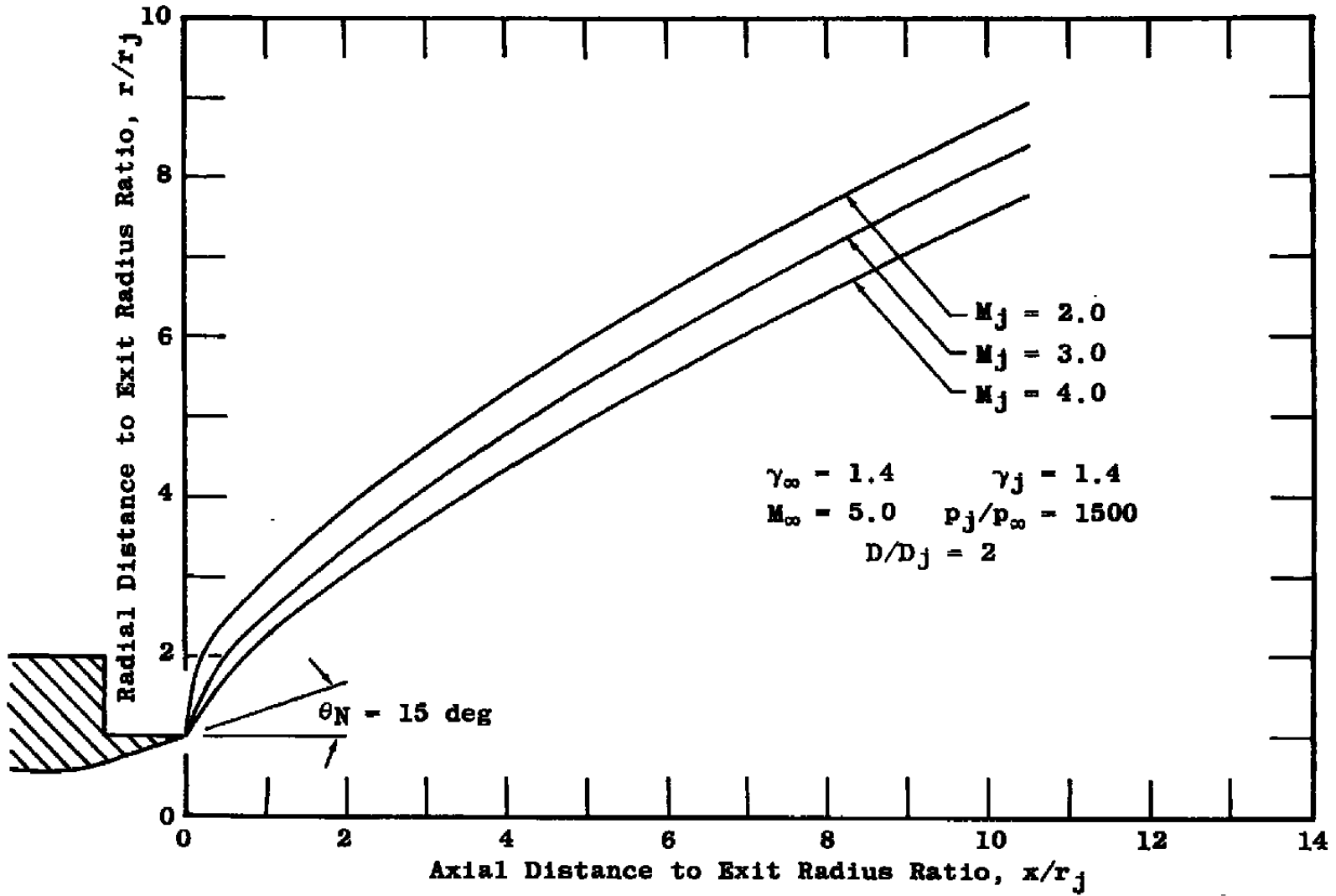
b. Configuration 2

Fig. 13 Concluded



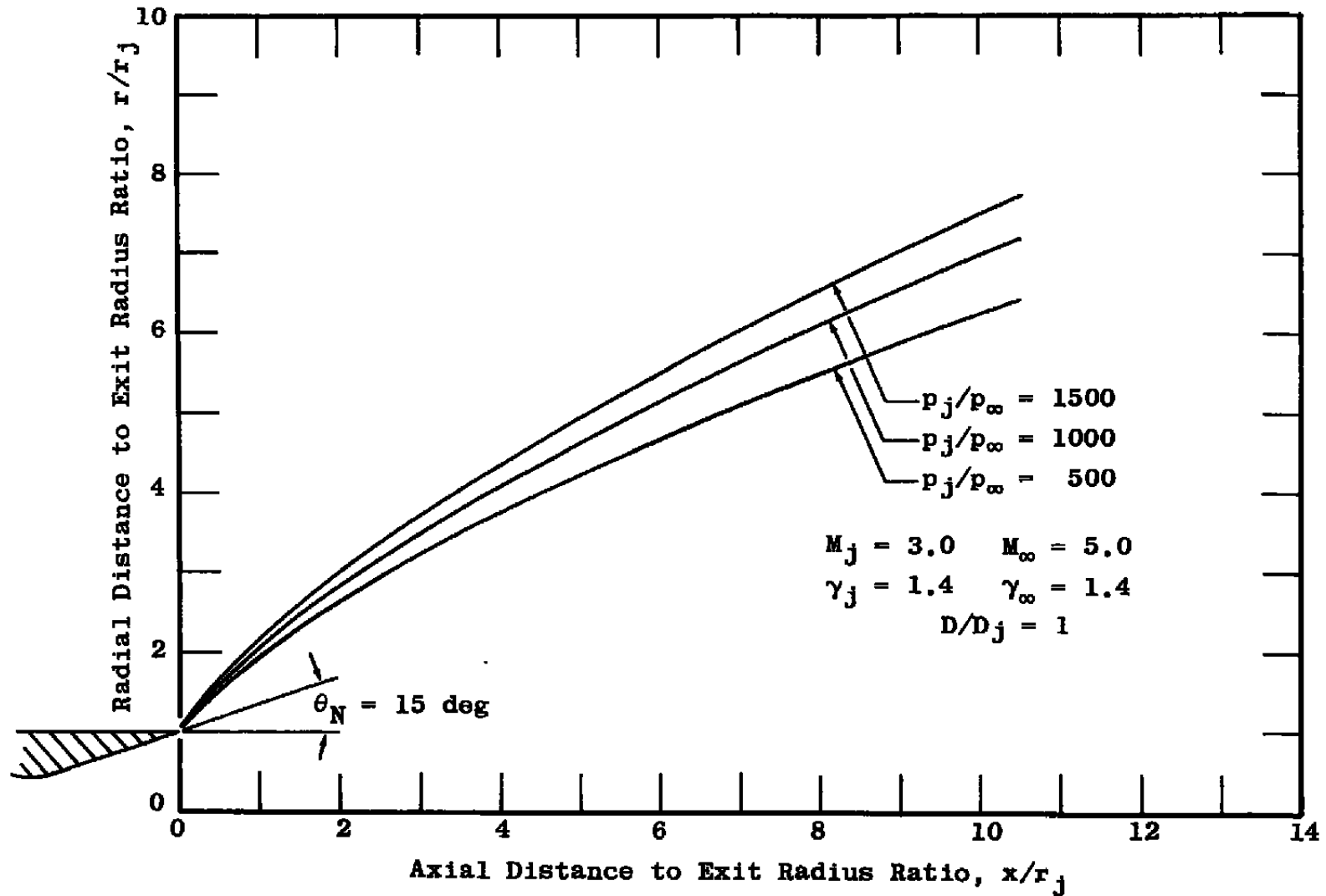
a. Configuration 1

Fig. 14 Jet Boundaries Calculated by the Present Hypersonic Method for Various Nozzle Mach Numbers



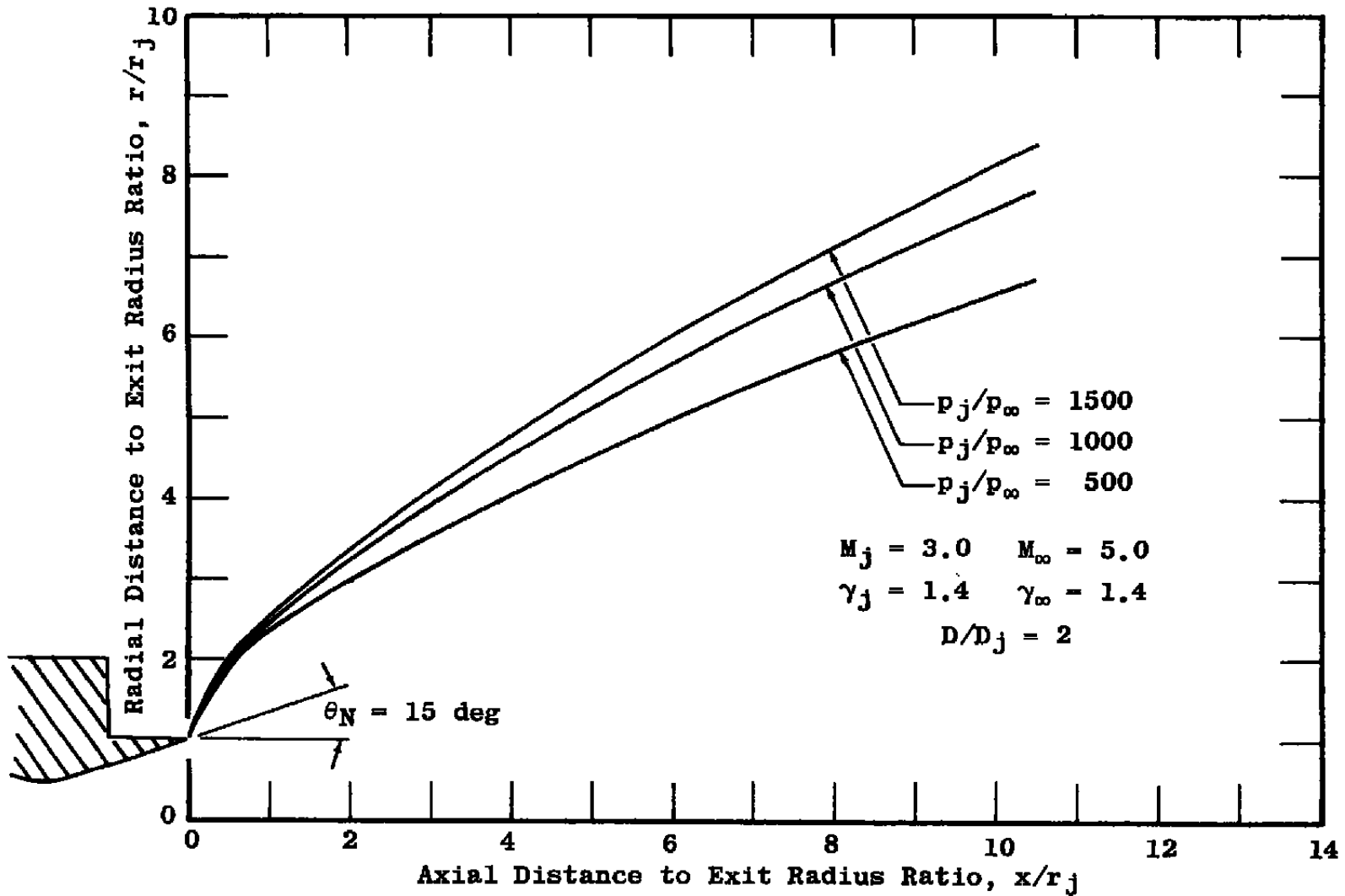
b. Configuration 2

Fig. 14 Concluded



a. Configuration 1

Fig. 15 Jet Boundaries Calculated by the Present Hypersonic Method for Various Static Pressure Ratios,  $p_i/p_\infty$



b. Configuration 2

Fig. 15 Concluded

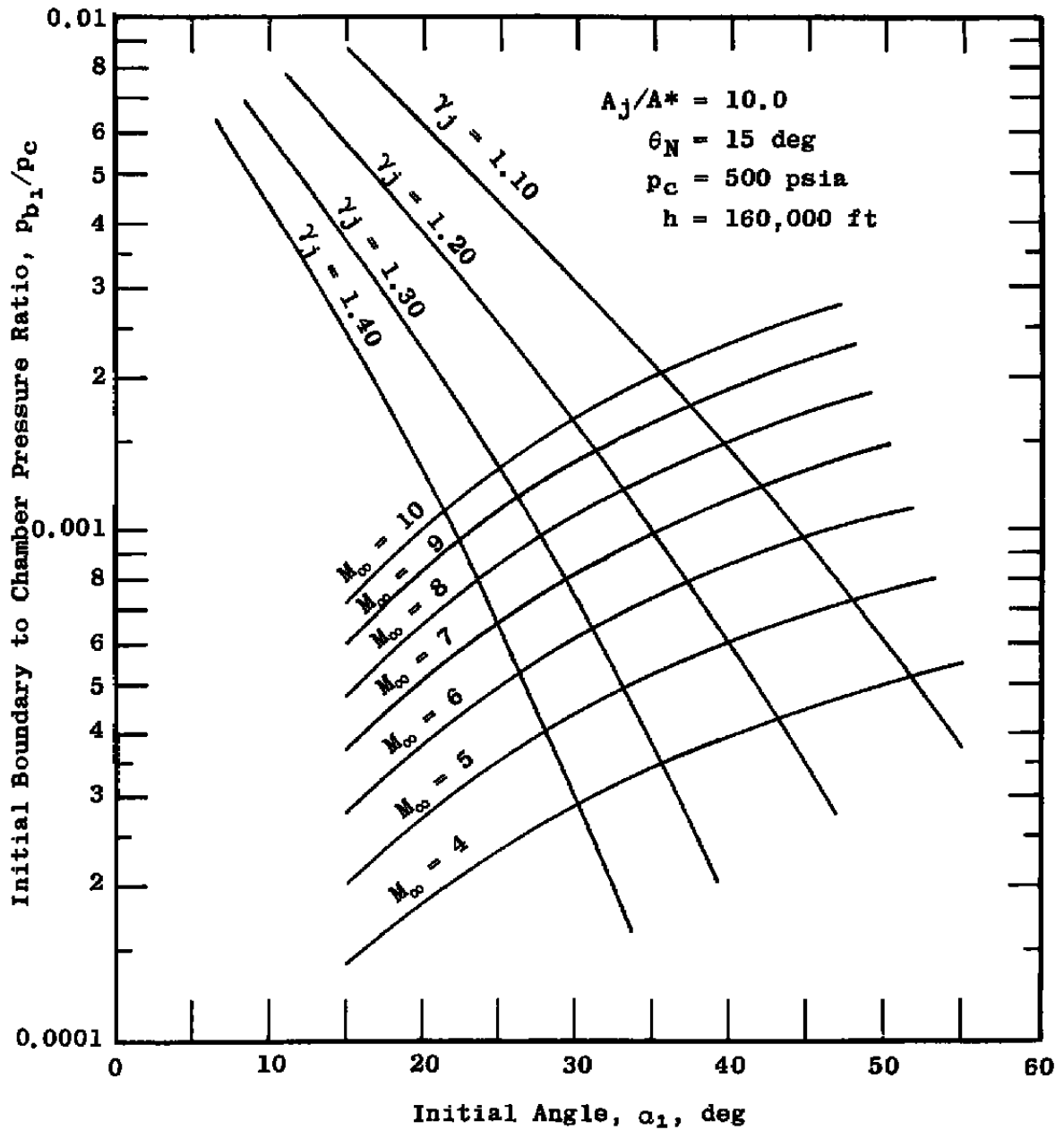
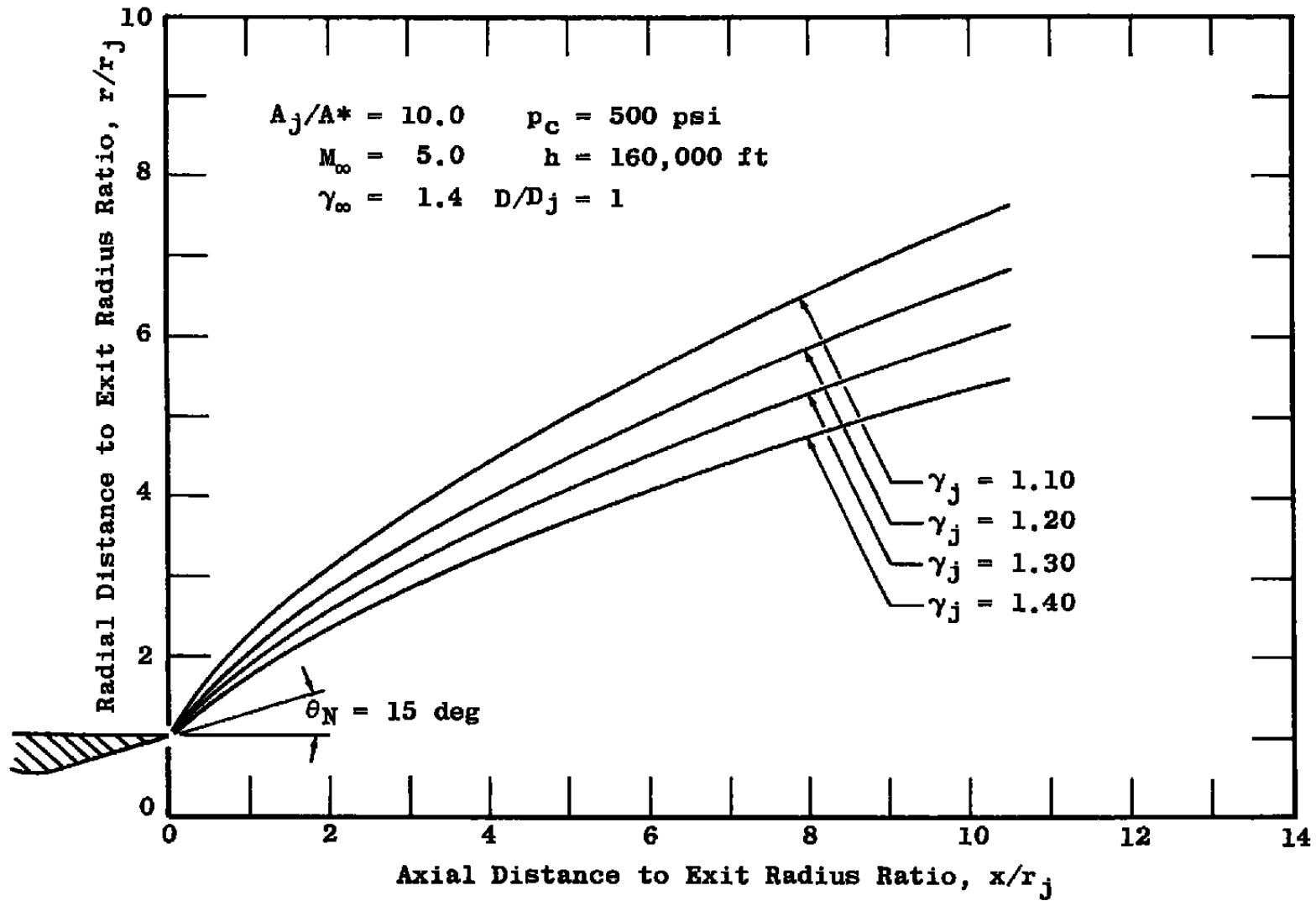
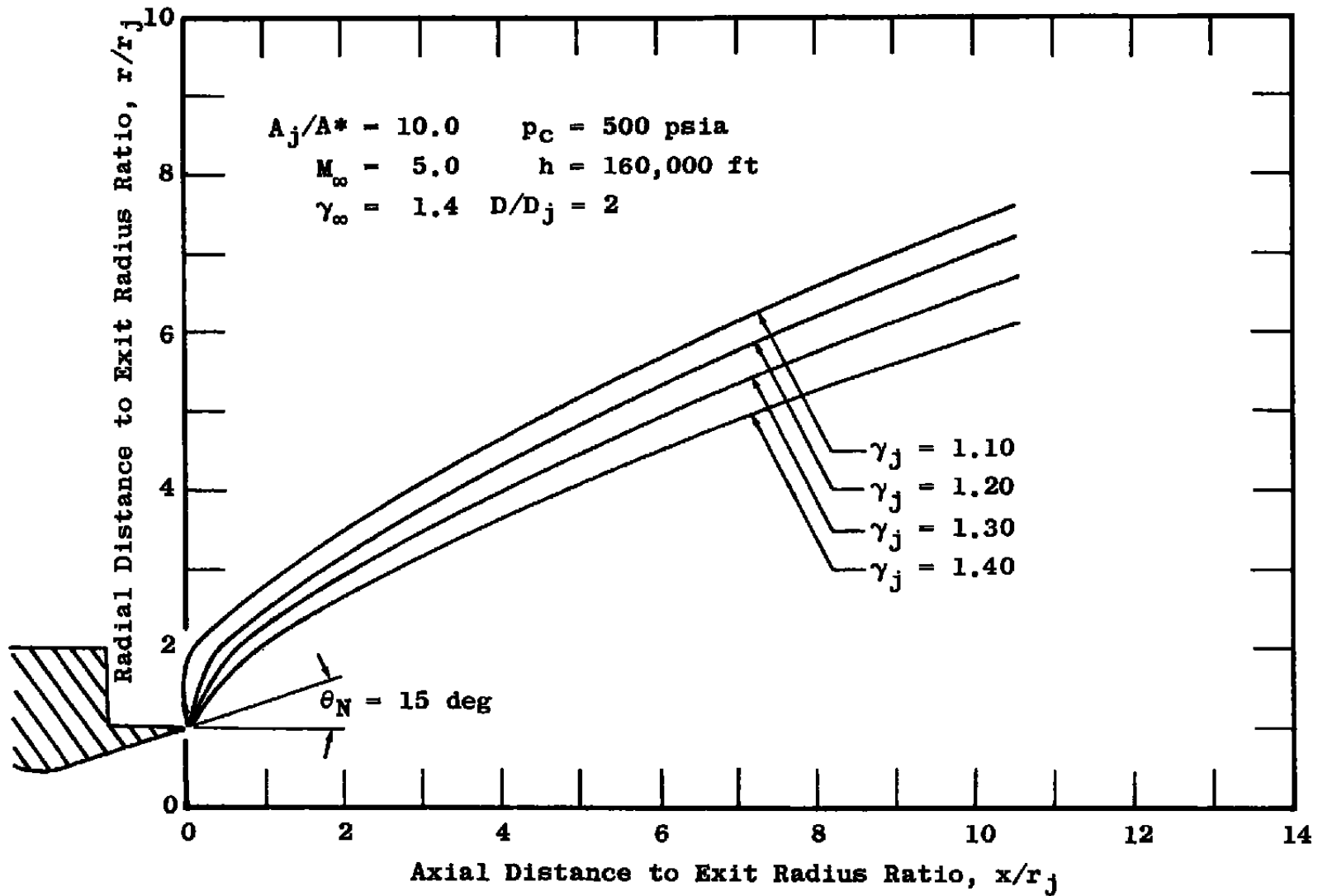


Fig. 16 Initial Angle Plot for Constant Nozzle Area Ratio, Chamber Pressure, and Free-Stream Altitude at Various Jet Specific Heat Ratios and Free-Stream Mach Numbers



a. Configuration 1

Fig. 17 Jet Boundaries Calculated by the Present Hypersonic Method for Various Jet Specific Heat Ratios



b. Configuration 2

Fig. 17 Concluded